ORIGINAL PAPER

CrossMark

Equatorially/globally conditioned meteorological analysis of heaviest monsoon rains over India during 23–28 July 2005

Ashwini Ranade[1] · Nityanand Singh[2]

Abstract

The heaviest monsoon rainstorm of the period 1951–2007 over India occurred during 23–28 July 2005, mostly the peninsula received rainfall, and each day the rainwater over the country was 40.0 bcm (billion cubic meter) or more, highest 98.4 bcm fell on 25 July 2005. Present premise of monsoon genesis is that it evolves in association with spreading and intensification of equatorial atmospheric condition over Afro-Eurasian landmass and adjoining Indian and Pacific Oceans during boreal summer. Robust natural criteria have been applied to demarcate monsoon and other global weather regimes (GWRs) at standard levels (1000−100 hPa). Global atmospheric (1000−100 hPa) thermal condition and monsoon and general circulations during 23–28 July 2005 have been compared with normal features of respective parameters. Over tropics-subtropics (45°S–45°N), troposphere (1000−250 hPa) was warmer-thicker and pressure lower than normal and mixed conditions of positive/negative departures in temperature, height/thickness and pressure over northern and southern mid-high latitudes. Noticeable changes in 3D monsoon structure were: horizontally spread and eastward-southward shifted over western North Pacific and stretched further southeastward across equatorial Pacific; intense warm-low lower tropospheric confluence-convergence across Asia–Pacific with vertical depth extending beyond 400 hPa; and intense warm-high upper tropospheric anticyclonic circulation zonally stretched and divided into three interconnected cells. Outflows from anticyclonic cells over Tibetan plateau and western North Pacific were mostly directed westward/southwestward/southward. Troposphere was warmer-thicker and pressure higher over eastern part of both subpolars-polars and cooler-thinner and pressure lower over western part. During the period, a deep cyclonic circulation moved from Bay of Bengal through central India while near-stationary atmospheric condition prevailed across the globe.

1 Introduction

Extreme monsoon rains cause severe flooding and disasters across India every year in some parts or the other, surprisingly, even during large-scale droughts, e.g. 1979. According to the National Commission on Floods, more than 40-million hectares of land of the country (total geographical area

✉ Ashwini Ranade
  ranadeashwini@gmail.com

  Nityanand Singh
  singhnityanand@gmail.com

[1] Present Address: Surface Water Hydrology Division, National Institute of Hydrology, Roorkee, Uttarakhand 247667, India

[2] Indian Institute of Tropical Meteorology, Dr. Homi Bhabha Road, Pashan, Pune, Maharashtra 411008, India

329 million hectares) are prone to floods. Every year about 7.5 million hectares of land is affected and 1600 lives lost (NDMG 2008). From elaborate analysis of 40 parameters of wet and dry spells and their extremes across India during 1951–2007, we understand that point/local, short duration extreme rain events (EREs) are embedded in large-scale, long-period moderate-to-heavy rainfall activities (area-averaged longer duration wet spell- each day rainfall intensity exceeded specified threshold) (Singh and Ranade 2010). There is widespread belief that recent global warming has affected the EREs across the country. A surge of studies has undertaken the problem of EREs across India (Goswami et al. 2006; Rajeevan et al. 2008; Guhathakurta et al. 2011; Ranade and Singh 2014 and references therein). Results of these studies corroborate widespread belief that the EREs would increase in the wake of global warming (IPCC 2007). Consensus among the current generation of coupled atmosphere–ocean general circulation models is that 'in a warmer climate, the intensity of extreme high-rainfall

would increase due to intensification of hydrological cycle resulting from warming at the surface and long-wave cooling higher in the atmosphere' (Senior et al. 2002). Hunt and Burgers (2002) have also emphasized the importance of studies on extreme precipitation variability in their philosophical commentaries. After general acceptance of global warming a reality, extreme rainfall studies have been undertaken mostly to generate information useful for assessment of hydro-meteorological disasters, as well as to respond to important issues raised by world scientific community. Some important regional studies on extreme precipitation/rainfall from across the world are Durman et al. (2001), Kharin and Zwiers (2000), Klein Tank et al. (2006), Zwiers and Kharin (1998), Kundzewicz et al. (1993) and many others.

Numerous studies have reported a characteristic change in extremes of short period rainfall of India (Sen Roy and Balling 2004; Goswami et al. 2006; Rajeevan et al. 2008; Goswami and Ramesh 2008; Ajayamohan et al. 2010 and many more). Ajayamohan et al. (2010) have attributed rising frequency in summer monsoon EREs over central India to a significant increase in synoptic activities. De and Dutta (2005) emphasized the role of convective instability in producing heavy rain spells over the Western Ghats. Francis and Gadgil (2006) have shown that most of intense rain producing systems over west coast are organized on synoptic and larger scales and are linked to atmospheric conditions over the equatorial Indian Ocean. Ranade et al. (2010) have identified development of seventeen synoptic scale convection-convergence zones that produce rainfall across Asia–Pacific region during active phases of the summer monsoon. Recently, the authors (Ranade and Singh 2014) have studied variations in spatio-temporal extreme rainfall fields over the Indian region. It is shown that point/local, short-duration EREs are embedded in large-scale, long-period intense heavy to very wet spells, and rainwater generated during main monsoon wet period is highly correlated with Asia–Pacific monsoon intensity. On 26–27 July 2005, unprecedented rainfall of 944 mm occurred over Mumbai metropolis (18°56′N, 72°51′E), located along West Coast between the Arabian Sea and Western Ghats. From synoptic and thermodynamic analyses of satellite-and-radar combined data, Shyamala and Bhadram (2006) concluded that formation of mesoscale convective systems comprised super thunderstorm cells, which interacted with synoptic scale low-pressure area from the Bay of Bengal, led to concentrated rainfall activities over Mumbai region. Due to enormous significance of this disastrous ERE, researchers have carried out simulation studies using different numerical weather prediction models (Bohra et al. 2006; Kumar et al. 2008; Rama Rao et al. 2007; Sikka and Rao 2008; Vaidya and Kulkarni 2007). The 2005 monsoon was near-normal, June–September rainfall was 99% of long-term mean. During the year, commencement phase of the

monsoon was rather weak, late and showed large variation during the season, July +14%, August −28% and September +17%. Ranade and Singh (2014) have examined features of large-scale wet spell and its extremes over India during 1951–2007. Each day 1°-grid cell was identified as wet if actual rainfall exceeded respective grid monsoon mean rainfall. Continuous period with each day more than 10.4% of the total area of the country under wet condition was demarcated as large-scale wet spell. Normally, the main monsoon wet spell over the country occurs from 18 June through 16 September (91 days). During the main monsoon wet spell, 26.5% area of the country experiences wet condition with rainfall intensity 26.3 mm/day and rainwater 20.2 bcm/day (billion cubic meter/day). During 2005, the monsoon wet spell occurred from 18 June through 27 August (71 days), duration was shorter than normal but the country experienced most severe 25-day spatio-temporal ERE concerning rainwater (Ranade 2010; Ranade and Singh 2014). Around 12 July 2005, monsoon circulation started strengthening with lower tropospheric convergence over Indian subcontinent extended up to 500 hPa, which persisted up to 20 August. During 21 July–7 August 2005, the monsoon was intense with a vertical depth of lower levels convergence extended up to 400 hPa—each day wet area of the country was more than 1.5 times the seasonal mean (26.5%) and rainwater more than the seasonal mean (20.2bcm). The monsoon was more vigorous during 23 July–28 July 2005, each day rainwater was 40.0 bcm or more (Fig. 1a, b). During the period, mostly peninsula experienced the wet condition. Most vigorous condition occurred on 25 July 2005, which produced 98.2 bcm of rainwater over the country. Point most extreme rainfall of 944 mm occurred at Mumbai recorded on 27 July 2005 but the country as a whole received lesser rainwater (54.4 bcm).

The nomenclature 'monsoon' is from the Arab spice traders for 'seasonal' (as 'annual event' or 'ritual') reversal of wind direction over northern Arabian Sea during summer from winter. During July, northwesterly over the Red Sea, its cyclonic curvature (turning to westerly flow) over the northern Arabian Sea and again a northwesterly wind along Indian West Coast (including Malabar region) favored forward journey, and during November, northeasterly over northern Arabian Sea turning to a southeasterly wind over the Red Sea favored backward journey for the sailors. However, from modern scientific analysis of elaborate global atmospheric data, a picture of the monsoon circulation is as: Monsoon is the largest thermally-direct tropical circulation which produces summer seasonal rainfall across Asia–Pacific. From an examination of isobaric level (1000–100) global chart of normal daily streamlines for the whole year, we understand that the monsoon evolves in association with spreading and intensification of equatorial atmospheric condition (warm, low and moist) over northern
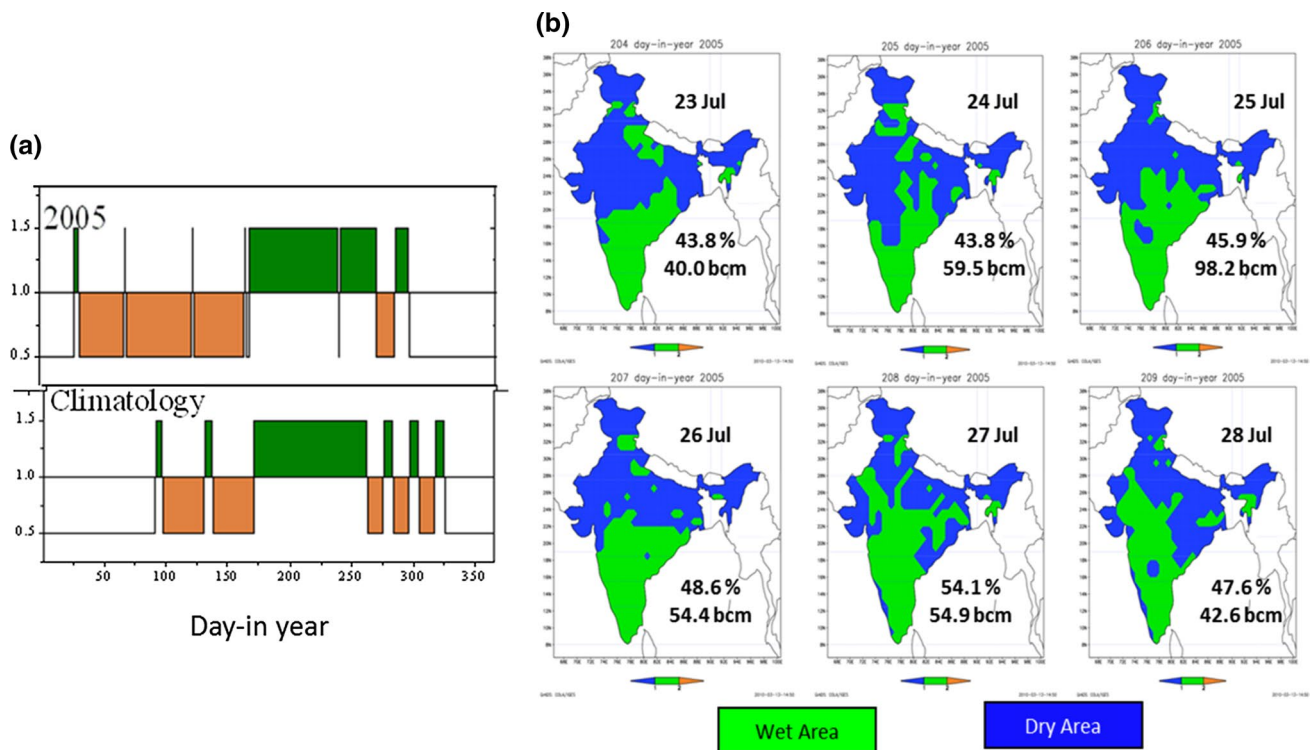
Fig. 1 **a** Climatology of sequence of large-scale wet and dry spells over India, and those of the year 2005, and **b** percentage area of India (PAI) under the wet and dry conditions, and rainwater (in bcm) during each of the 6 days of heaviest rainstorm (23–28 July 2005)

hemisphere (NH) during boreal summer. The process starts during end-March and reaches full maturity during end-July when the global atmospheric thermal structure (boreal summer, austral winter, north–south thermal contrast and hot period over Tibet) attains its peak. At maturity, 3D structure of the monsoon circulation is as: deflected Indo-Pacific easterlies in the lowest layer up to 850 hPa while sweeping entire Indian subcontinent flow northeastward and eventually join Aleutian subpolar convergence zone; Eurasian temperate westerlies in the layer 850 and 500 hPa enter the Indian subcontinent through Middle-East sector and evolve into a giant whirlpool-type cyclonic circulation over Indian subcontinent with extended trough (convergence) zone across Indo-Gangetic plains; and evolution of upper tropospheric anticyclonic circulation in layers 300–100 hPa, originating over eastern Tibet and growing westward to cover whole of subtropical Afro-Eurasia and North Atlantic, resembles like east–west oriented Thermal Mountain Range. Indian monsoon evolves as a component when the Asia–Pacific monsoon attains adequate strength (say end-May).

The deflected Indo-Pacific easterlies penetrate through a wide range of thermal, moisture and wind regimes (tropical, subtropical, temperate and subpolar), therefore, cause generation of variety of secondary perturbations (point, line, trough, meander, circular, elliptical, wave and front), which eventually produce the rainfall. Effects of Coriolis force, orography and

diabetic heating contribute considerably to monsoon circulation, cloud formation and rainfall mechanism. Subregional/local factors alter the monsoon system (large-scale features, embedded secondary perturbations and rainfall processes) in a complex way. Broadly, basic nature of the monsoon is tropical but characteristics of its secondary disturbances are wide-ranging, equatorial through subpolar, which gives rise to idea of subregional monsoons. Recently, Ranade et al. (2010) have identified 18 subregional monsoons. Earlier, Ramage (1971) observed distinctly different features of the Asian monsoon circulation across three subdivisions west of 70°E—middle-tropospheric subsidence, large vertical wind shear and fine weather; between 70°E and 105°E—large-scale upward motion, large vertical wind shear, monsoon depressions, subtropical cyclones and frequent rains; and east of 105°E—intermittent upward motion, small vertical wind shear, typhoon, subtropical cyclones and changeable weather. Qian and Lee (2000) have divided monsoon into six subregional interlinked monsoons (Indo-China Peninsula monsoon, South China Sea monsoon, South Asian monsoon, East Tibet Plateau monsoon, East Asian monsoon and Northeast Asian monsoon). By end-May, spreading of intense equatorial atmospheric condition covers South China Sea, southeastern China, Indochina, eastern Tibet and Bay of Bengal with vertical depth of convergence extending up to 700 hPa. By end-June, the convergence extends up to 600 hPa over entire Indian subcontinent, and

by end-July, up to 500 hPa over Arabian Sea, India, southern Tibet, Bay of Bengal and Indochina. At 600 hPa, however, spreading is over larger spatial domain than at 500 hPa, and the entire Asia–Pacific region at 700 hPa. In other words, Indian monsoon can be regarded as core component and others sub-regional/local monsoons within the ambit Asia–Pacific monsoon circulation. Definite quantitative picture of the monsoon circulation does not seem to exist, even normal picture, leave aside real-time and 3-dimensional structure. Few large-scale, long-period heavy rain events occur over India during every monsoon. But location, orientation, shape, size, and intensity of the monsoon structure appears to be considerably different during these events. The purpose of the present investigation is to understand 3D features of the Asia–Pacific monsoon and global atmospheric thermal as well as circulation structures during unprecedented wet spell of 23–28 July 2005. Four main objectives of the study are:

1. to demarcate monsoon as well as other global weather regimes by applying robust natural criteria;
2. to describe effectively normal 3D global atmospheric thermal and monsoon as well as general circulations during 23–28 July;
3. to describe departure from normal in scalar atmospheric parameters, and actual monsoon as well as general circulations during the heaviest rainstorm over the country (23–28 July 2005); and
4. to investigate impact of rainstorm period monsoon changes, if any, on global atmosphere thermal condition and general circulation.

2 Dataset used

Global atmospheric data and Indian rainfall for the period 1979–2013 have been utilized in the present study. Daily (6-hourly mean) 2.5°-gridded mean sea level pressure (mslp) and precipitable water (PW), and temperature, geopotential height and wind (u and v) at 12 standard isobaric levels (1000–100 hPa) are obtained from 'The National Centers for Environmental Prediction (NCEP)/Climate Forecast System Reanalysis (CFSR/CFSv2)' (Saha et al. 2010, 2014). Details of daily 0.5°-gridded rainfall of India are given in Rajeevan and Bhate (2008).

3 Delineation of global weather regimes (GWRs)

Climatological literature provides qualitative description of seasonal spatio-temporal variation (shift, intensification, weakening, restructuring, etc.) in global precipitation zones (e.g. Strahler 2011). According to form, amount and seasonality in precipitation occurrences, eleven zones can

be identified in global precipitation field: north and south polar high (sparse precipitation in all seasons), north and south subpolar low (ample precipitation in all seasons), north and south mid-latitude wavy westerlies (winter wet, summer dry), north and south subtropical high (dry in all seasons), north and south tropical (summer wet, winter dry) and equatorial low (abundant rainfall in all seasons). Tropics receive seasonal rainfall from weather systems that evolve from spreading and intensification of equatorial low during respective hemisphere summer, and mid-latitudes receive precipitation from equatorward spreading/shifting/intensification of subpolar low during respective hemisphere winter. Atmospheric changes over the two hemispheres are broadly opposite during most times of the year. Temperature and geopotential height are important parameters to understand basic nature of any weather system. Considering effectively conditioned isobaric level (1000−100 hPa) temperature and height, a quantitative approach for classification of large-scale weather regimes across the globe has been attempted. Corresponding equatorial mean value (EMV) (mean of 2.5°S–2.5°N across the globe) has been used as a reference due to its inherent characteristics, i.e. seasonality is least and diurnal variation a minimum. Table 1 gives annual mean and standard deviation of temperature and height at standard isobaric levels (1000−100 hPa) over the equator. Equatorially conditioned (grid-cell value minus EMV) temperature (EC-T_{level}) and geopotential height (EC-Z_{level}) at particular level has been considered as two attributes (positive and negative) and arrived at the following four types of broad or large-scale weather regimes.

1. *Warm-low regime ($EC\text{-}T_{level} > zero\ and\ EC\text{-}Z_{level} < zero$)* Convergence/confluence (inflow) with fast-rising motion in lower levels and slow sinking in upper levels.
2. *Cool-low regime ($EC\text{-}T_{level} < zero\ and\ EC\text{-}Z_{level} < zero$)* Convergence/confluence (inflow) with slow-rising motion in lower levels and fast sinking in upper levels.
3. *Warm-high regime ($EC\text{-}T_{level} > zero\ and\ EC\text{-}Z_{level} > zero$)* Divergence/difluence (outflows) with slow-rising motion in lower levels and fast-rising in upper levels.
4. *Cool-high regime ($EC\text{-}T_{level} < zero\ and\ EC\text{-}Z_{level} > zero$)* Divergence/difluence (outflow) with fast sinking motion in lower levels and slow sinking in upper levels.

Annual mean of mslp and wind speed (*W*) over the equator is not robust like temperature and geopotential height/thickness, and neither the two parameters (mslp and *W*) display general downward slope from equator-to-pole. However, the global mean value (GMV) of mslp (Table 2) and *W* (Table 1) is found robust. The isolines of globally conditioned *W* (GC-W) have been displayed on the chart showing weather regimes across the globe. Parallel comparison of normal daily chart of equatorially conditioned

Table 1 Annual mean (and annual standard deviation, SD) of normal daily equatorial mean value (EMV, zonal average over 2.5°S–2.5°N) of temperature and geopotential height/thickness at isobaric levels (1000–100 hPa) as well as whole troposphere (1000–250 hPa), and that of normal daily global mean value (GMV) of horizontal wind speed

Level (hPa)	Tropospheric (°C)		Tropospheric height/thickness (m)		Wind speed (m/s)	
	Annual EMV	Annual SD	Annual EMV	Annual SD	Annual GMV	Annual SD
1000	26.1	0.4	93.0	6.1	4.2	0.2
925	21.2	0.5	774.4	5.3	5.2	0.2
850	17.2	0.3	1502.9	4.6	5.3	0.2
700	8.7	0.2	3135.5	4.0	6.3	0.2
600	2.6	0.3	4398.5	4.1	7.4	0.2
500	−5.1	0.2	5823.0	25.3	9.0	0.3
400	−16.0	0.2	7570.4	5.6	11.2	0.5
300	−31.8	0.3	9670.6	7.7	14.7	0.7
250	−41.9	0.3	10931.7	9.2	16.7	0.7
200	−54.0	0.3	12402.4	10.9	18.2	0.6
150	−67.8	0.2	14187.0	12.2	17.6	0.4
100	−79.6	1.9	16542.0	12.7	13.2	0.6
T_{TROP}	−2.1	0.3	10838.7	12.3	8.9	0.3

mslp (EC-mslp) and globally conditioned (GC-mslp) for the whole year did not show any significant difference. Therefore, the EC-mslp will be used here as it is consistent with the basic premise of the present study, 'Asia–Pacific monsoon evolves in association with spreading and intensification of equatorial atmospheric condition'. No genuine reason is seen to condition wind direction; therefore, unconditioned chart of streamlines has been prepared during the analysis. Equatorially conditioned precipitable water (EC-PW) has been used in the study wherever required. The above classification can be detailed by incorporating EC-mslp and EC-PW for identification of zonal/regional weather systems, e.g. low or high pressure under warm or cool condition (equatorial or subpolar low), and further wet or dry condition (tropical or

Table 2 Normal tropospheric temperature T_{TROP} (EC-T_{TROP}) and thickness Z_{TROP} (EC-Z_{TROP}) and mslp (EC-mslp) during 23–28 July over indicated geographical domains, and departure from normal during 23–28 July 2005

Geographical domains	Tropospheric temperature T_{TROP} (°C)		Tropospheric thickness Z_{TROP} (m)		mslp (mb)	
	Normal (EC-T_{TROP})	Departure	Normal (EC-Z_{TROP})	DFN	Normal (EC-T_{TROP})	Departure
GLB (globe)	−9.7 (−7.1)	+ 0.5	10514.7 (−305.5)	+ 23.3	1011.4 (−0.3)	+ 0.2
NH (north hemis.)	−4.9 (−2.4)	+ 0.6	10704.0 (−116.1)	+ 25.7	1012.0 (0.4)	0
SH (south hemis.)	−14.4 (−11.9)	+ 0.5	10325.4 (−494.8)	+ 20.8	1010.7 (−1.0)	+ 0.4
NPL (north polar) (70°–90°N)	−22.7 (−20.2)	+ 0.9	10214 (−605.5)	+ 54.6	1010.8 (−0.9)	+ 5.2
NMLat (north mid-lats.) (45°–70°N)	−11.0 (−8.5)	+ 0.2	10460.2 (−360.0)	+ 4.1	1011.8 (0.1)	+ 0.8
TSBT (tropic–subtropic) (45°S–45°N)	−5.0 (−2.5)	+ 0.8[5%]	10704.2 (−115.9)	+ 32.5[10%]	1014.3 (2.7)	− 0.8
SMLat (south mid-lats.) (45°–70°S)	−26.7 (−24.2)	− 0.3	9811.8 (−1008.4)	− 11.1	995.6 (−16.1)	+ 2.8
SPL (south polar) (70°–90°S)	−41.1 (−38.6)	− 0.5	9291.3 (−1528.8)	− 18.7	1001.4 (−10.2)	+ 6.8
TBT (Tibet) (27.5°–7.5°N; 65°–95°E)	5.3 (+ 7.8)	+ 0.6	10987.9 (+ 167.8)	+ 22.3	1005.1 (−6.6)	− 0.3
WW-TBT (west–west TBT) (27.5°–37.5°N; 55°–75°E)	4.3 (+ 6.9)	0	10996.4 (+ 176.3)	+ 3.8	1002.9 (−8.7)	+ 1.2
W-TBT (west TBT) (27.5°–7.5°N; 65°–75°E)	4.2 (+ 6.8)	+ 0.4	11002.5 (+ 182.3)	+ 7.2	1001.8 (− 9.8)	0
C-TBT (central TBT) (27.5°–7.5°N; 75°–85°E)	7.4 (+ 9.9)	+ 0.7	10985.3 (+ 165.2)	+ 22.9	1005.8 (− 5.8)	− 0.5
E-TBT (east TBT) (27.5°–37.5°N; 85°–95°E)	6.3 (+ 8.8)	+ 0.8	10976.0 (+ 155.8)	+ 36.9	1007.6 (−4.1)	− 0.5
EE-TBT (east–east TBT) (27.5°–37.5°N; 95°–105°E)	3.9 (+ 6.5)	+ 1.0	10944.4 (+ 124.3)	+ 41.9	1008.2 (−3.5)	− 0.5

EC indicates equatorially conditioned value

extratropical). It can be further detailed by assigning class-interval to positive and negative equatorially/globally conditioned values of the parameters.

After wind generation, other causes of convergence are: Coriolis, orographic and frontal effects, collision/confluence of two or more air flows, channelization of large flow, cyclonic curvature/circulation or U-turn flow, trough in wavy flow, etc., and divergence: difluence/spreading of large flow, lee-side subsidence, cold air mass incursion, anticyclonic curvature/circulation, ridge in wavy flow, etc. A negative value of the GC-W indicates cyclonic or anticyclonic curvature/circulation and weak intensity, and positive straight-flowing strong wind. Therefore, display of streamlines and isotach (GC-W) superimposed on the chart of weather regimes would be helpful to visually gauge intensity of different weather systems (including location and intensity of jet stream) as well as to differentiate two or more systems of the same basic nature (lows or highs) in different climatic zones. We believe that warm-low, warm-high and cool-high regimes may be collectively referred to as barotropic regime, and cool-low as baroclinic regime. Different weather regimes will be collectively referred to as general or global weather regimes (GWRs). All the four regimes may not occur all times at all the isobaric 'levels', it could be two or three also. When both the hemispheres are in thermally near-balanced state (end-March), cool-low and cool-high regimes occupy most areas on the GWRs chart of 925 hPa (not shown). Tropical-subtropical areas experience cool-high condition, mid-high latitudes cool-low condition, and only limited area around the equator and low latitudes warm-low and warm-high conditions. By considering EC-mslp in two attributes (positive and negative) in the GWR classification, it is simple to differentiate equatorial/tropical low from subpolar-polar low, and subtropical high from polar high. The EC-PW can be used to delineate precipitation regimes, i.e. snowfall, rainfall. Tropical seasonal rainfall regime or monsoon regime can be demarcated by incorporating two additional conditions in the classification, i.e. EC-mslp negative and EC-PW positive. It will be only a minor refinement of warm-low regime discussed in the beginning.

4 Troposphere and upper levels

Examination of level-wise normal daily global charts of the equatorially-conditioned temperature (EC-T_{level}) for the whole year revealed the following:

1. From 1000 hPa through 250 hPa, large parts of the hemisphere (particularly land areas) experience warmer-than-equator condition during respective peak summer—spreading is slightly larger in the lower levels (say up to 50°N parallel in the NH and 40°S parallel in SH:

southern hemisphere), and lesser in upper levels (say 45°N in the NH and 20°S in the SH); and subpolar-polar regions of both the hemispheres are cooler-than-equator throughout the year. For the 23–28 July period, global distribution of normal EC-T_{level} at four selected levels (1000, 700, 400 and 250 hPa) is shown in Fig. 2.

2. At 200 and 150 hPa levels, the atmosphere over subpolar-polar regions is warmer-than-equator during respective summer, and cooler during winter (23–28 July chart shown in Fig. 3).

3. At 100 hPa, however, most parts of the NH are warmer-than-equator throughout the year. Large parts of the SH were also warmer throughout the year but polar region experienced cooler condition during austral winter (or Indian monsoon). Indo-Pacific region is cooler throughout the year, while South Asia, Arabian Sea and Africa experience cooler conditions during monsoon (Fig. 3).

Due to close similarity in level-wise spreading and intensification of equatorial temperature condition, the layer between 1000 and 250 hPa will be considered as troposphere in the study, and 200, 150 and 100 hPa as upper levels. This is only to optimize vertical description of the global EC-T field rather than to demarcate upper boundary of the atmosphere for monsoon studies. Important to note that upper tropospheric anticyclonic circulation of the monsoon system is fully developed at 200, 150 and 100 hPa levels. Using arithmetic mean of nine levels between 1000 and 250 hPa as tropospheric temperature (T_{TROP}), normal daily global chart of EC-T_{TROP} for the whole year has been examined and found well-organized, distinctly different and uniquely intense evolution of thermal field over Asia–Pacific and surrounding regions during boreal summer. Outside this huge and thermal field (EC-T_{TROP} positive), the atmospheric is cooler-than-equator (EC-T_{TROP} negative), coolest being south polar. Within the warmer region, equatorially-conditioned height (EC-Z_{level}) of lower tropospheric levels is negative and upper tropospheric levels (up to 100 hPa) positive. The EC-T_{level} of all the levels is negative outside the warm region. Examination of normal daily global field of the EC-Z_{TROP} (Z_{TROP}, tropospheric thickness equal to Z_{250} minus Z_{1000}) reveals that there is close parallelism in the EC-T_{TROP} and EC-Z_{TROP} fields throughout the year, which is understandable. The two fields are expected to provide useful information about the general direction of large-scale air flows. Further, it is our endeavour to understand relationship of monsoon with large-scale winds in upper levels (200, 150 and 100 hPa) where equator-to-pole temperature slope reverses over NH and deepens over SH.

In the following two sections, normal and actual features of 3D global atmospheric thermal condition and monsoon and general circulations during the storm period (23–28 July 2005) have been described in order. Equatorially/
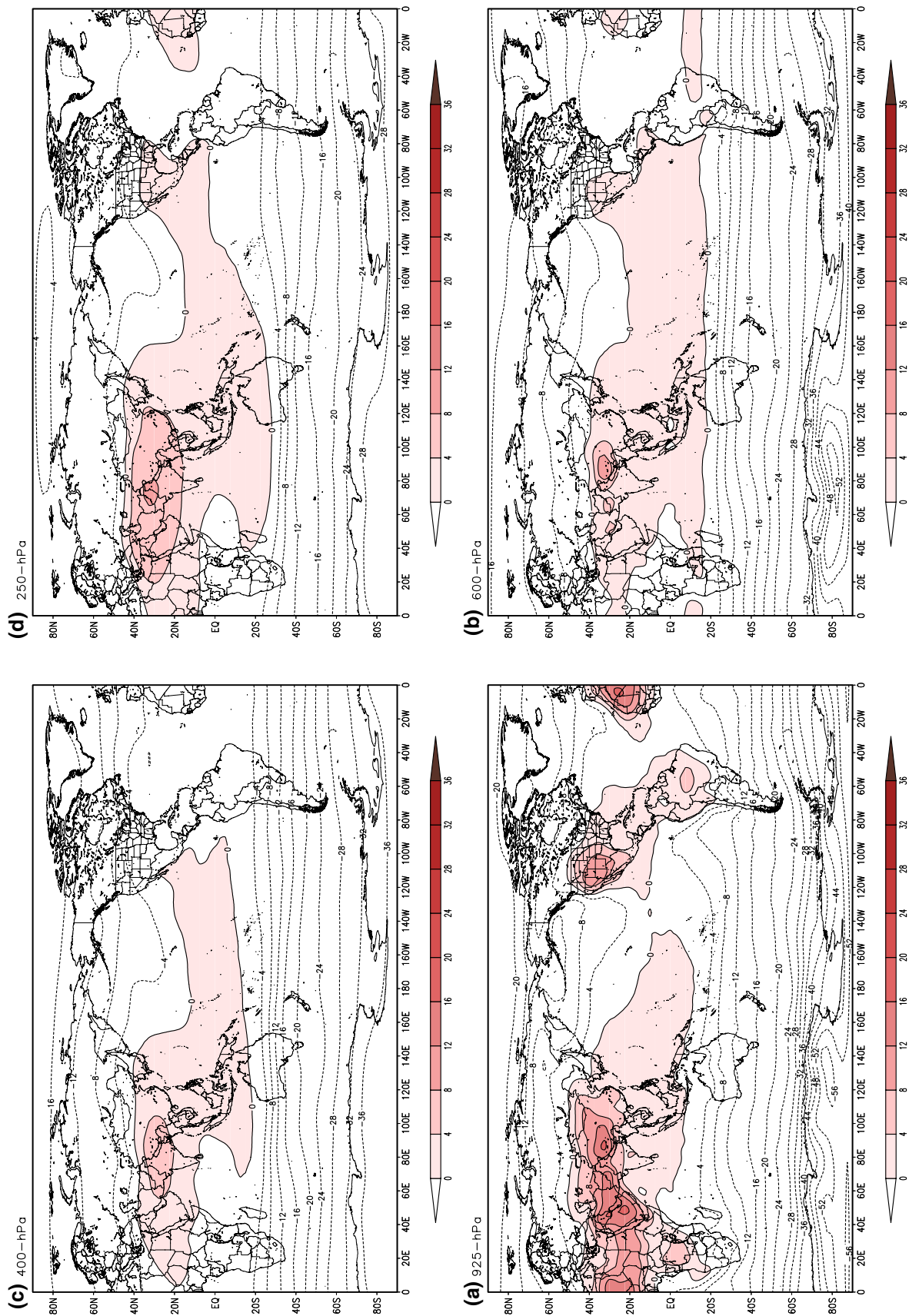
Fig. 2 Global distribution of normal 23–28 July equatorially conditioned temperature at four selected levels, 925-hPa (EC-T_{925}) (**a**), 600-hPa (EC-T_{600}) (**b**), 400-hPa (EC-T_{400}) (**c**) and 250-hPa (EC-T_{250}) (**d**). Isolines are in °C, and red shading indicates EC value positive, and unshaded negative
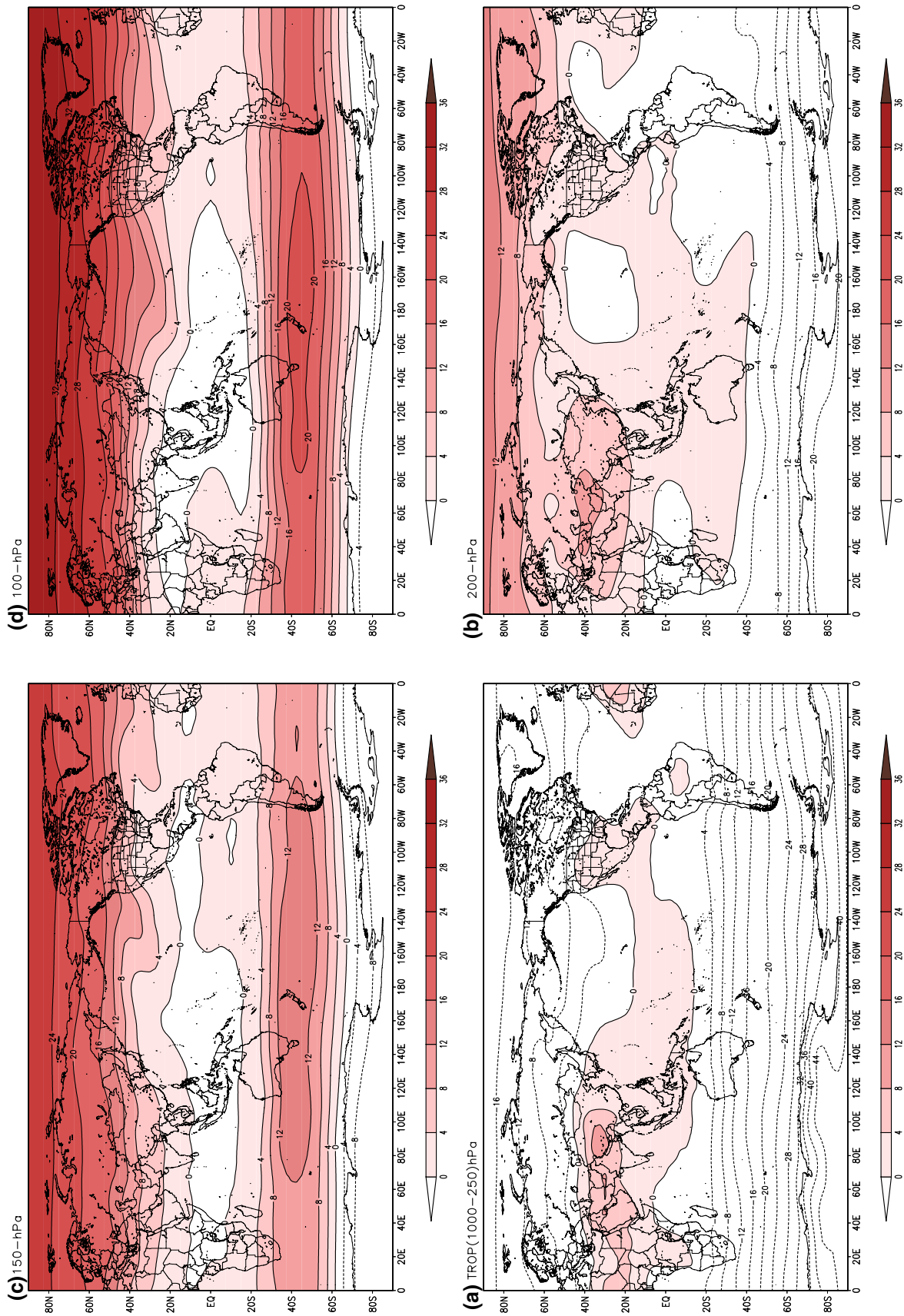
Fig. 3 Chart of 23–28 July showing global distribution of normal equatorially conditioned tropospheric temperature (EC-T_{TROP}) (**a**), and temperature of upper levels: EC-T_{200} (**b**), EC-T_{150} (**c**) and EC-T_{100} (**d**). Isolines are in °C, and red shading shows EC positive, and unshaded EC negative

globally-conditioned value of the parameters (excluding streamlines) have been considered for describing normal features and departure-from-normal for actual features.

5 Normal 3D structure of global atmospheric thermal condition and monsoon and general circulations during 23–28 July

5.1 Global distribution of equatorially-conditioned (EC) normal temperature, geopotential thickness/height, mslp and PW during 23–28 July

5.1.1 Normal EC-T_{TROP}, EC-T_{200}, EC-T_{150} and EC-T_{100}

Highest EC-T_{TROP} occurs over Tibetan region (+8 °C), decreases to less than −16 °C over north polar and −44 °C south polar (Fig. 3). To generate broad picture of global tropospheric temperature structure keeping Tibet at the core, area-averaged EC-T_{TROP} has been calculated for the globe, the two hemispheres and five broad climatic zones, tropic-subtropic, north mid-latitudes, south mid-latitudes, north polar and south polar, as well as five broad divisions across Tibetan region (Table 2). Tropospheric temperature contrast is least between Tibet and tropic-subtropic (+10.3 °C) and most between Tibet and south polar (+46.4 °C) (Table 3). The contrast between Tibet and north polar is +28.0 °C. The EC-T_{200} is positive across almost entire global area north of 30°S parallel. It increases to greater than +12 °C over north polar and decreases to less than −20 °C south polar. At 150-hPa, equatorial belt over Pacific, southeast Asia, Indian Ocean and Africa experiences cooler condition (negative EC-T_{150}). The EC-T_{150} increases to +24 °C over north polar and decreases to less than −8 °C over south polar. Large portions of western tropical Pacific (20°S–20°N) and south-southeast Asia and tropical Africa (10°–20°N) experience negative EC-T_{100} condition. The warmer condition occurs over almost entire NH, and the EC-T_{100} exceeds +32 °C over north polar. Further, a warmer condition also occurs over south mid-latitudes with core value greater than +20 °C but decreases to less than −4 °C over south polar. Cause of upper level warming has been explained in Subsect. 5.2.

5.1.2 Normal EC-Z_{TROP}, EC-Z_{200}, EC-Z_{150} and EC-Z_{100}

Global pattern of the EC-Z_{TROP} is similar to that of the EC-T_{TROP} (Fig. 4). Thickest troposphere occurs over Indo-Gangetic plains—Persian Gulf sector (> +200 m). Contour value of the EC-Z_{TROP} decreases to less than -500 m over north polar and −1800 m south polar. Area-averaged EC-Z_{TROP} over Tibet is +149.1 m (Table 2). Tropospheric

Table 3 Normal tropospheric temperature and thickness downward slopes from Tibet (TBT) to indicated geographical domains during 23–28 July, and departure from normal during 23–28 July 2005

Downward slope	Tropospheric temperature slope (°C)		Tropospheric thickness slope (m)	
	Normal	Departure	Normal	Departure
TBT-GLB	14.9	+ 0.1	473.2	− 0.9
TBT-NH	10.2	0	283.9	− 3.4
TBT-SH	19.7	+ 0.2	662.6	+ 1.5
TBT-TSBT	10.3	− 0.1	283.7	− 10.2
TBT-NMDLat	16.3	+ 0.4	527.7	+ 18.2
TBT-SMDLat	32.0	+ 1.0	1176.2	+ 33.5
TBT-NPL	28.0	− 0.2	773.3	− 32.3
TBT-SPL	46.4	+ 1.2	1696.6	+ 41.0

For abbreviation and geographical boundary see Table 2

thickness contrast is least between Tibet and tropic-subtropic (273.5 m) and most between Tibet and south polar (1737.6 m) (Table 3). The contrast between Tibet and north polar is 741 m. The core of positive EC-Z_{200} (> +100 m) is located over eastern China-Libya sector, and zonally oriented pattern decreases to less than −600 m over north polar and −1800 m south polar. Positive core of EC-Z_{150} (> +200 m) is located over Eastern Tibet–Syria sector, the field value decreases to less than −500 m over north polar and −2000 m south polar. Prominently large positive core of the EC-Z_{100} (> +200 m) is over eastern China—eastern Mediterranean sector, less than −100 m over north polar and −2000 m south polar. In upper levels, core area is larger northward and westward over Afro-Eurasia.

5.1.3 Normal EC-mslp

A hugely large EC-mslp negative field (EMV is 1011.6 mb) occurs over the NH (almost entire Asian continent, western-and-equatorial North Pacific, eastern Africa, north polar and eastern Canada) with core less than −12 mb over Indo-Gangetic plains (Fig. 5a). This contiguous low-pressure field is surrounded by positive EC-mslp fields of North Pacific, North Atlantic, Greenland and southern subtropic (all spatially well connected), each with core exceeding +10 to +12 mb. Circumpolar south subpolar negative EC-mslp field is wide and intense with multiple cores of less than −32 mb across. South polar positive EC-mslp field is large and intense with core value greater than +20 mb.

5.1.4 Normal EC-PW

Positive EC-PW field (EMV is 41.4 mm) is heavily concentrated across western North Pacific between parallels 15°S−40°N and east-southeast-south Asia with core greater
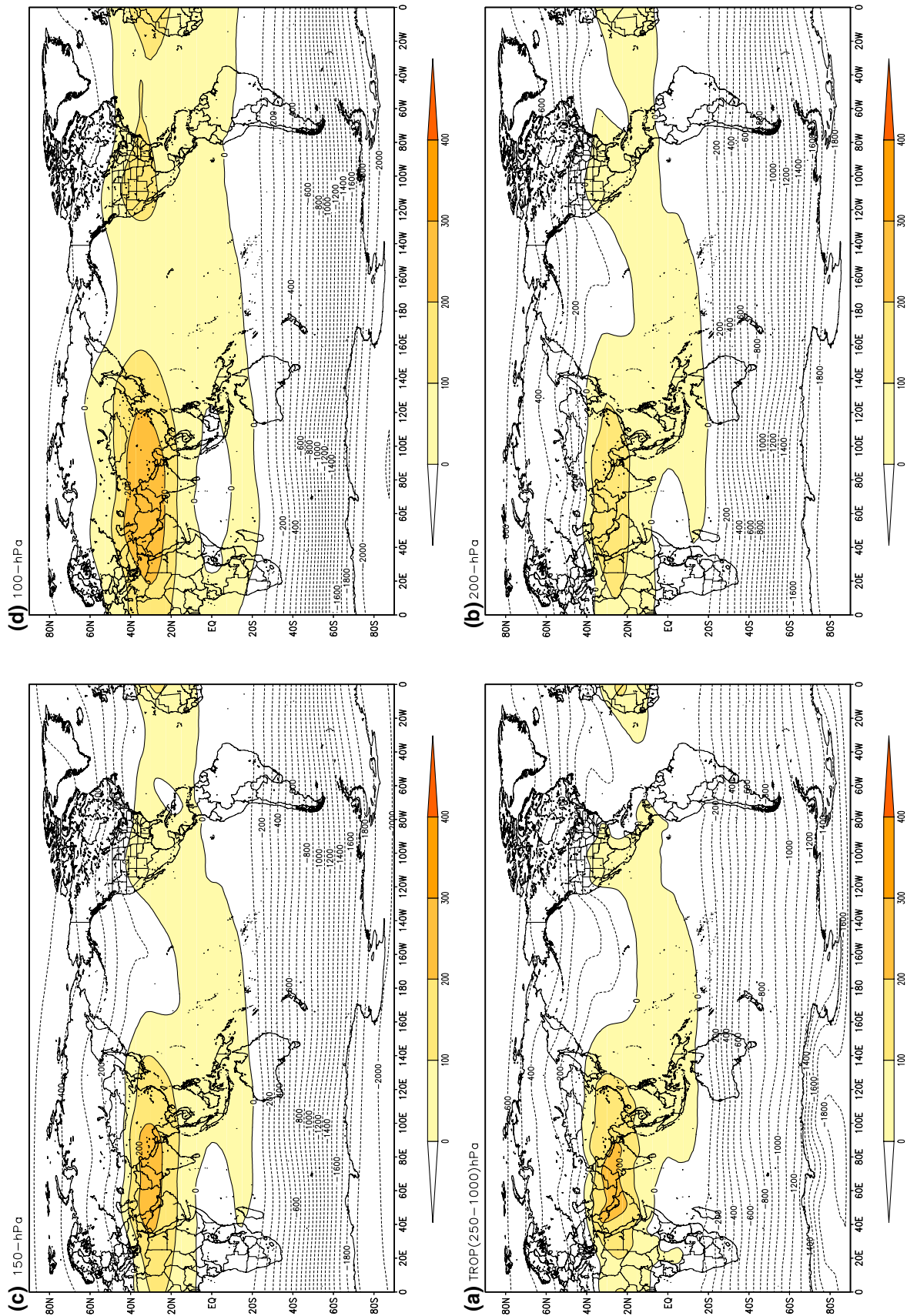
Fig. 4 Same as in Fig. 3 but for EC-Z_{TROP} (**a**), EC-Z_{200} (**b**), EC-Z_{150} (**c**) and EC-Z_{100} (**d**). Isolines are in 'm', and yellow shading shows EC-positive, and unshaded EC-negative
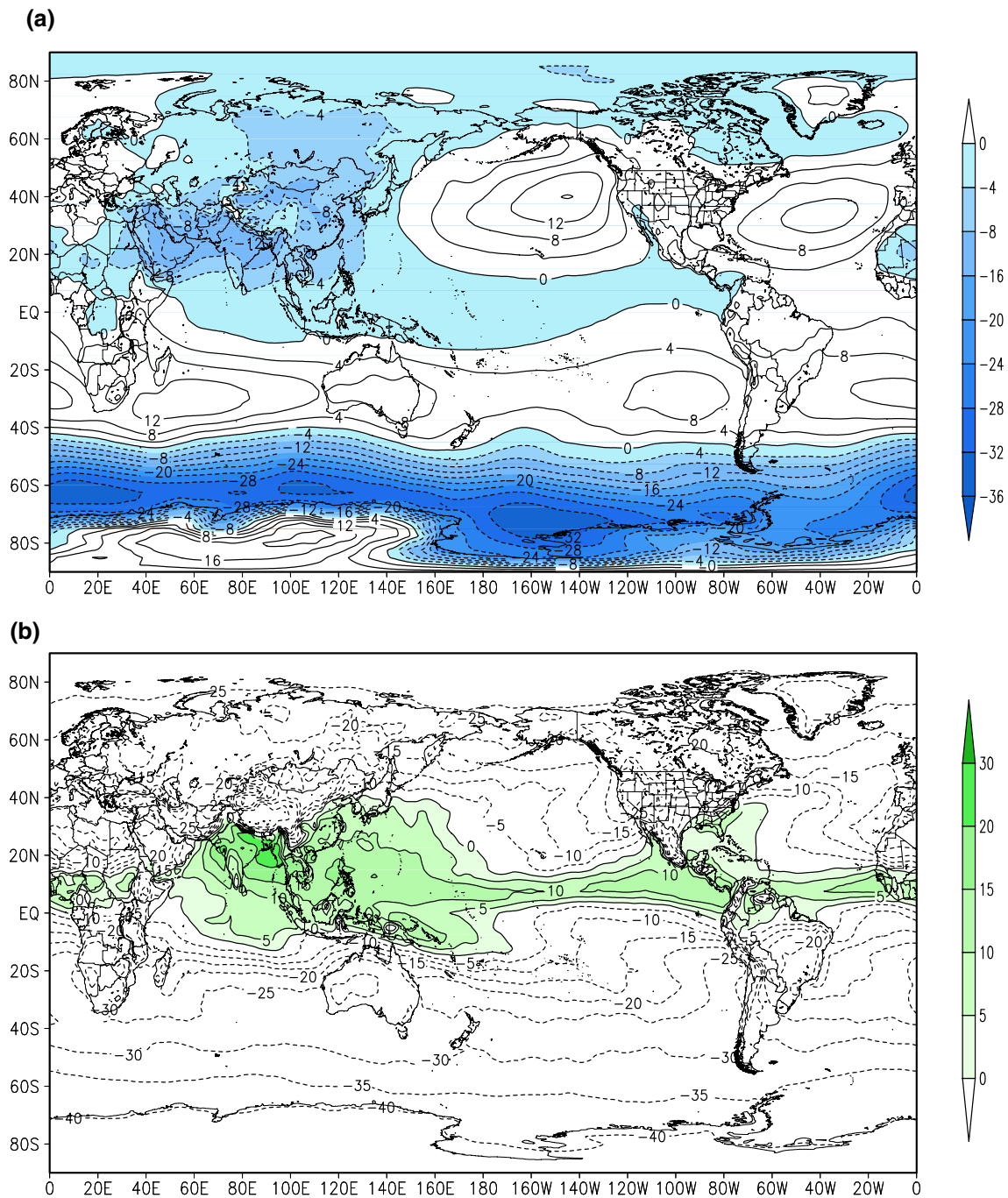
(a)

(b)

Fig. 5 Chart of 23–28 July showing global distribution of normal, equatorially conditioned mslp (EC-mslp) (**a**) and precipitable water (EC-PW) (**b**). In **a**, isolines are in mb, and blue shading shows EC-mslp negative, and unshaded EC-mslp positive; and in **b** isolines are in mm, green shading shows EC-PW positive, and unshaded EC-PW negative

than $+20$ mm located over the head Bay of Bengal and eastern-northeastern India (Fig. 5b). The field extends across equatorial Pacific, tropical America, equatorial Atlantic and north tropical Africa with cores greater than $+5$ to $+10$ mm. Negative field value occurs over polar regions, less than -25 mm over north polar and -40 mm south polar.

5.2 Normal monsoon and other GWRs, streamlines and GC-*W* during 23–28 July

At four selected levels (925, 600, 400 and 150 hPa) normal GWRs, streamlines and GC-*W* of the period 23–28 July have been shown in Fig. 6 for extended Asia–Pacific region (for a closer view of monsoon), and Fig. 7 for the

globe. Description, however, will tandemly shift from one figure to another. Charts of other levels are also kept in mind while describing the 3D structure of monsoon and general circulations.

Largest and most intense warm-low regime occurs across Afro-Eurasia/Indo-Pacific region (5°S–50°N; 20°E–150°E). Up to 850 hPa, deflected Indo-Pacific equatorial-tropical easterlies sweep the entire Asia–Pacific region. Between 850 and 500 hPa levels, Eurasian temperate westerlies enter into Indian subcontinent through Middle East sector as north-westerlies and evolve into a giant whirlpool-type cyclonic circulation over India and adjoining Arabian Sea and Bay of Bengal. Intensity of this cyclonic circulation varies with 3D structure and intensity of thermal field as well as the location of warmest core over dry-and-highlands of subtropical Afro-Asia. Across entire warm-low regime of Asia–Pacific, confluences/collisions occur between deflected warm-moist Indo-Pacific easterlies and cool-dry Eurasian westerlies-turned-northwesterlies. The warm-high condition is prominent over tropical-subtropical Americas and somewhat subdued around margin of the warm-low regime (Figs. 6, 7). The cool-high condition is a robust feature of North Pacific high, North Atlantic high and entire south subtropical high-pressure zone. The cool-low condition normally occurs over geographical domain north of 50°N as well as south of 40°S. From 1000 to 500 hPa level, size of warm-low and cool-high decreases and that of warm-high increases. In 400−250 hPa layer, warm-low regime ceases and size of warm-high increases further and cool-high decreases. At 200 hPa and above, northern cool-low regime changes to warm-low while size of the warm-low increases over south midlatitudes and that of cool-low decreases over south subpolar-polar.

Accumulation of rising airs from warm-low convergences around Tibetan region produces largest, thickest warm-high regime in the upper troposphere over subtropical Asia. The outflows from the anticyclonic circulation are distributed in three directions, west-southwestward, southward and north-northeastward. West-southwestward directed outflows while subsiding over northern Africa and North Atlantic turn right (anticyclonic curvature) and join north temperate westerlies which blow over Eurasia. In the layer 850−500 hPa, part of the Eurasian westerlies enters into monsoon domain through Middle East sector. Part of that flows eastward and collides and converges with deflected Indo-Pacific easterlies across Tibet-China-Japan sector. Remaining north midlatitude westerlies blow over North Pacific–North America–North Atlantic sector, take anticyclonic curvature from eastern side of north subtropical highs, join the Indo-Pacific easterlies and eventually return to warm-low regime of the Asia–Pacific. Outflows directed north-northeastward subside via cyclonic circulation over Arctic Ocean (north of Russia–Alaska–Canada sector) and an anticyclonic circulation evolves on the surface underneath. Heat advected by

Fig. 6 Chart of 23–28 July showing normal distribution of GWRs▶ (color shaded), streamline and wind speed (GC-*W* in m/s, red isolines) at 925-hPa (**a**), 600-hPa (**b**), 400-hPa (**c**) and 150-hPa (**d**) levels over extended Asia–Pacific (20°S–55°N; 25°E–135°W). Green shading shows *WL* warm-low regime; orange shading shows *WH* warm-high regime; white shading shows *CH* cool-high regime; blue shading shows *CL* cool-low regime

the outflows appears to be the main cause of warmer upper levels over the NH (Fig. 3). Return-flows from lower level of anticyclonic circulation via meander flow join the Indo-Pacific easterlies and eventually converge into the warm-low regime. Major portion of the outflows are directed southwards. Unsubsided outflows from north polar due to reversal of equator-to-north polar thermal slope and weakening of height slope also get merged with the south-bound outflows. While passing between Tibetan high and equatorial high as upper tropospheric easterlies, the combined outflows experience channelization effect and an important component of the monsoon, Tropical Easterly Jet (TEJ), is produced which blow over Bay of Bengal, equatorial Indian Ocean and Africa. In core of the TEJ at 150 hPa the GC-*W* exceeds + 10 m/s. After crossing the equator, the outflows partly subside via anticyclonic circulation over south subtropical high and remaining via cyclonic circulation over south polar. The return-flows from subtropical and polar highs via Indo-Pacific easterlies and south-north cross-equatorial flows converge into the monsoon warm-low regime. Horizontal wind across the entire NH is weaker than the equator, i.e. the GC-W is − 5 to − 10 m/s at all levels indicating cyclonic/anticyclonic curvature/circulation in the wind across the hemisphere. Over south subtropic-midlatitudes, the wind is greater than equator. The GC-W exceeds + 5 m/s in the core area of the 1000 hPa. It increases in the vertical and exceeds + 30 m/s at 250 hPa and above.

6 Departure from normal in global thermal condition and monsoon and general circulations during 23–28 July 2005

6.1 Global distribution of departures in actual temperature, geopotential thickness/height, mslp and PW on 23–28 July 2005

6.1.1 Departure in T_{TROP}, T_{200}, T_{150} and T_{100}

Broadly troposphere was warmer (positive departure) across the entire tropic-subtropic and large parts of north mid-high latitudes (Fig. 8). On the other hand, large parts of south mid-high latitudes experienced cooler (negative departure) condition. Departure in area-averaged T_{TROP} over tropic-subtropic was + 0.8 °C, significant at 5% level according
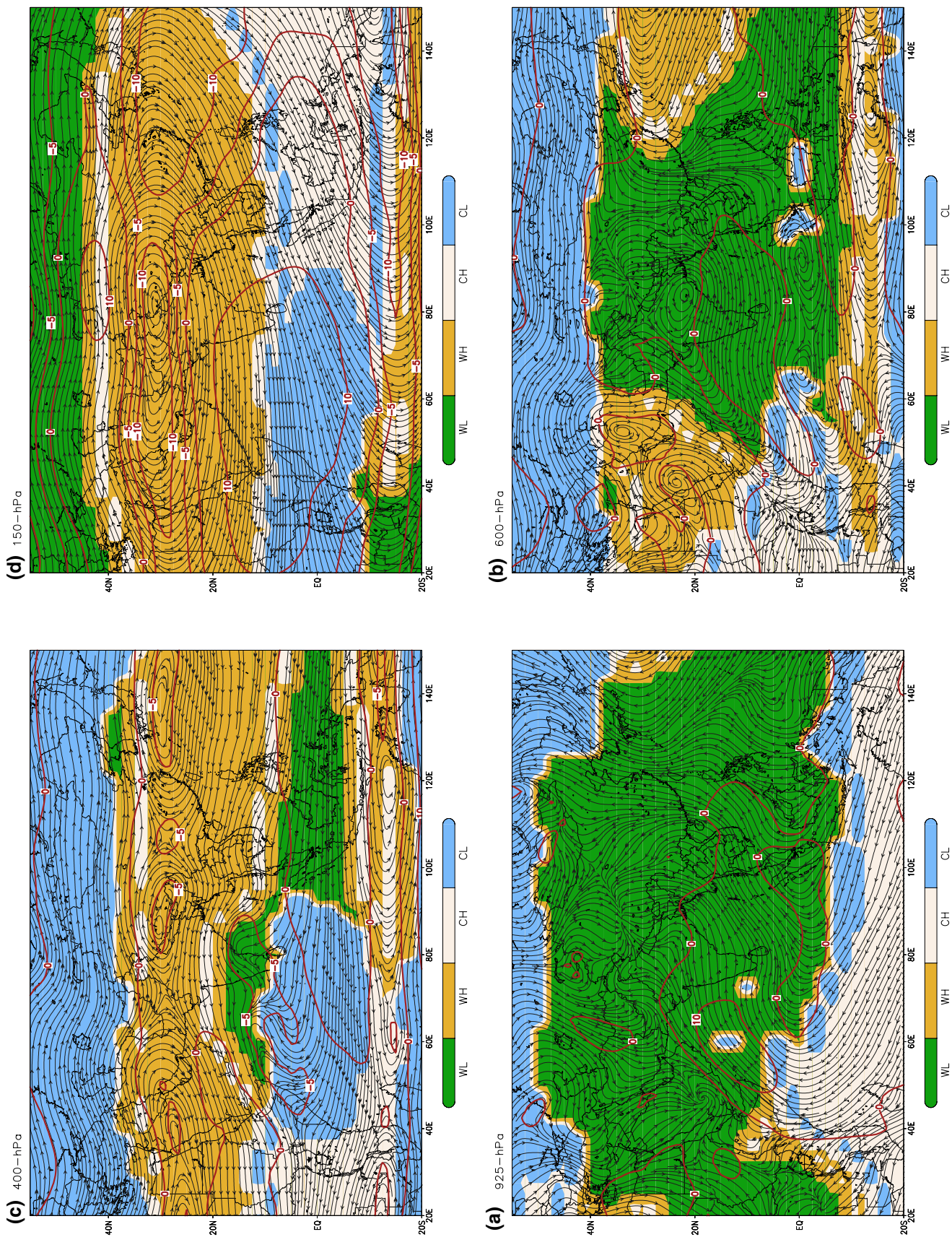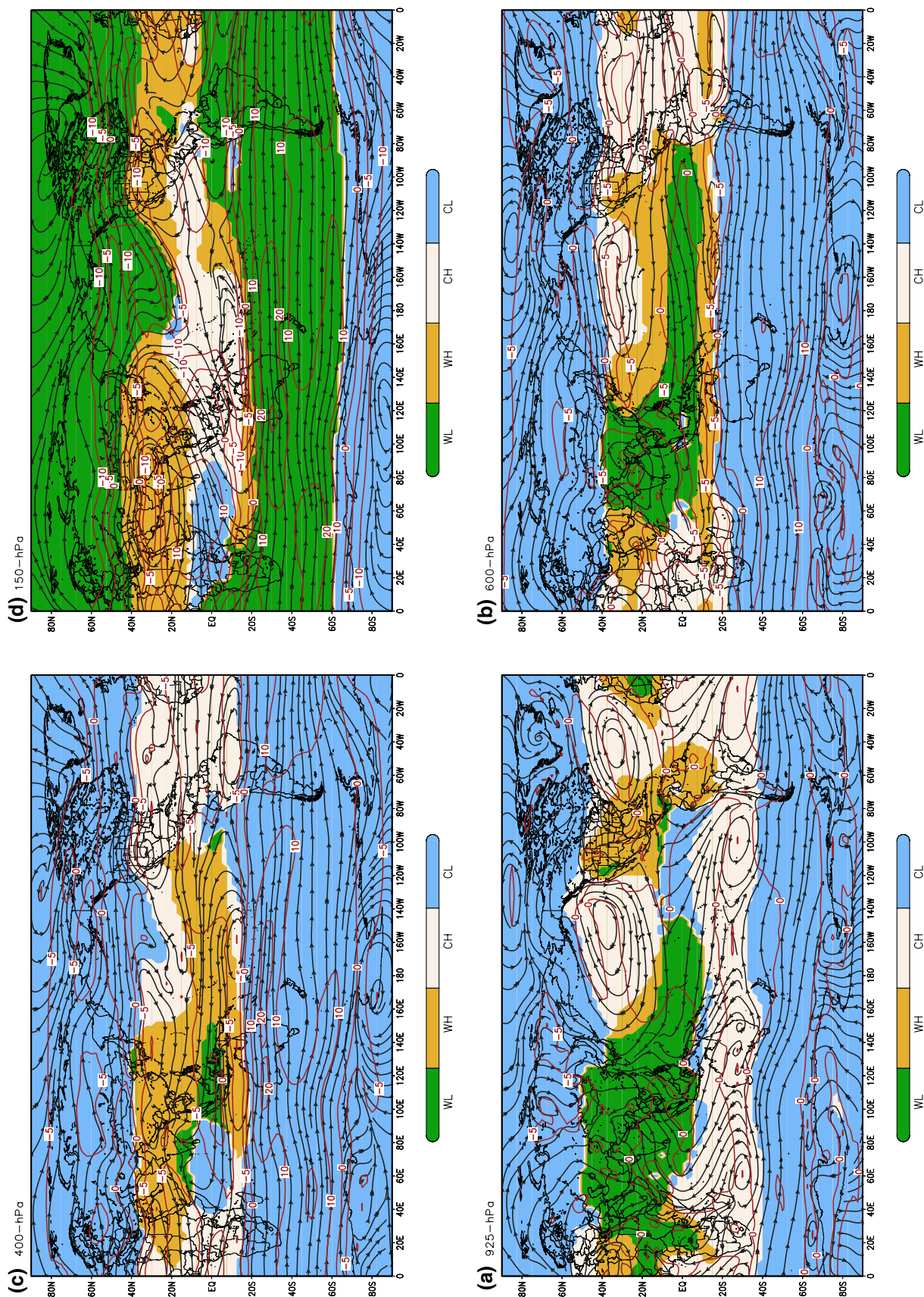
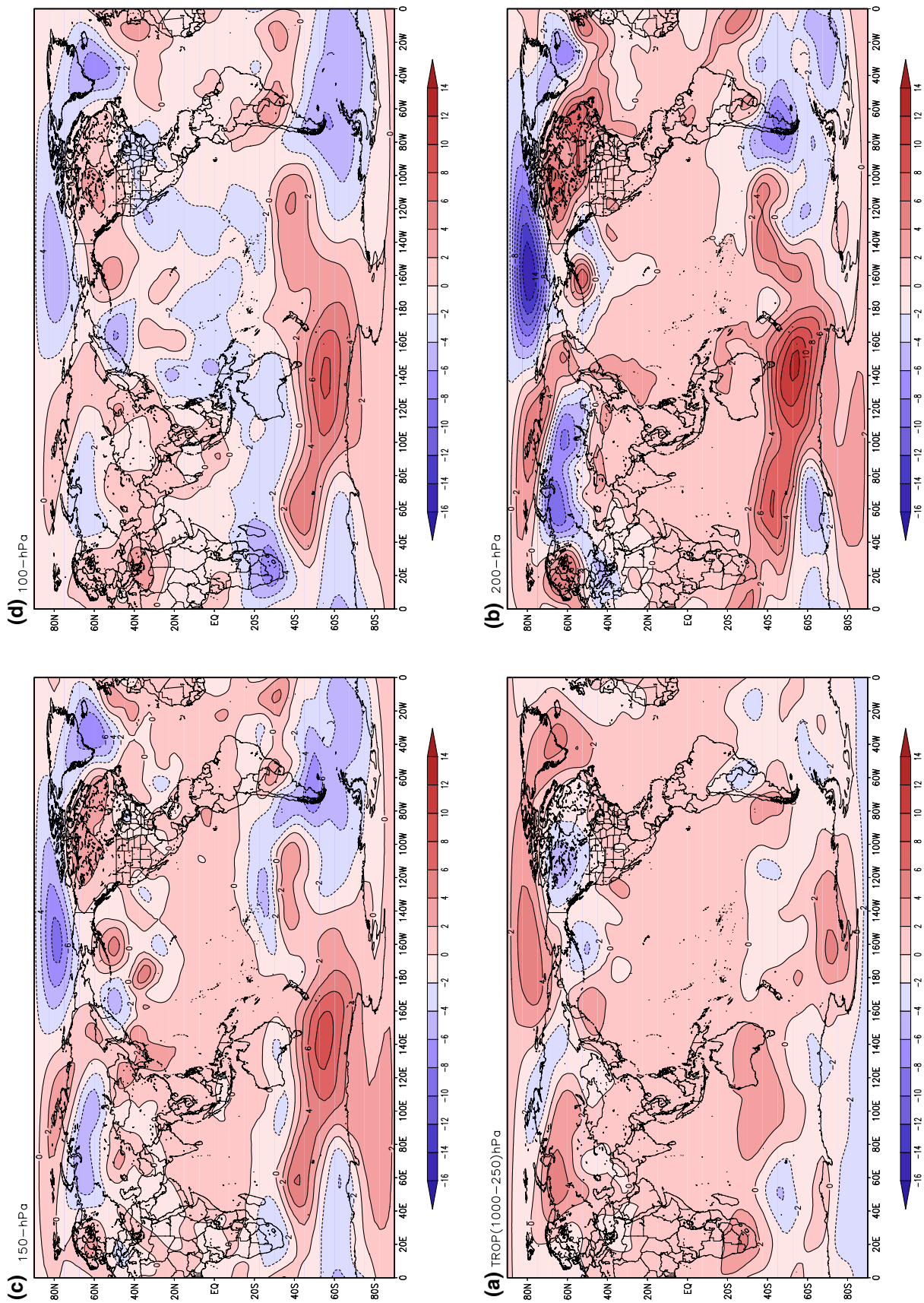**Fig. 7** Same as in Fig. 6 but over the globe

Fig. 8 Chart of 23–28 July 2005 showing global distribution of departure from normal in tropospheric temperature (T_{TROP}), and that of temperature of the upper levels (T_{200}, T_{150} and T_{100}). Isolines are in °C, and red shading shows positive departure, and blue negative departure

to Student's *t* statistic test (Table 2). Troposphere was over north mid-latitudes ($+0.2$ °C) and north polar ($+0.9$ °C). Warmer atmosphere occurred over lesser part of tropic-subtropic at 200- and 150-hPa, and cooler over larger parts at 100 hPa. In the upper levels, cooler condition occurred over large parts of north mid-high latitudes and warmer over south mid-high latitudes.

6.1.2 Departure in Z_{TROP}, Z_{200}, Z_{150} and Z_{100}

Departure in Z_{TROP} was positive over large parts of tropic-subtropic and north mid-high latitudes, and negative over large parts of south mid-high latitudes (Fig. 9). Departure in area-averaged Z_{TROP} over tropic-subtropic was $+32.5$ m (significant at 10% level), north midlatitudes $+4.1$ m, north polar $+54.6$ m, south midlatitude -11.1 m and south polar -18.7 m (Table 2). Global pattern of departure in height of the upper levels was similar to that of the tropospheric thickness.

6.1.3 Actual global field of EC-mslp

Intense lower-than-equator mslp (EC-mslp negative) field around Tibetan plateau was well organized and had extension over northern Africa, northwestern North Pacific (core south of Japan) and equatorial Pacific. Isolated intense negative EC-mslp field occurred over Scandinavia, northern Russia, and northwestern USA–Canada–Baffin Sea sector (Fig. 10a). This negative EC-mslp field was surrounded by hugely large positive EC-mslp field that stretched from 40°S parallel to entire north polar with cores of $+10$ to $+16$ mb across subtropical and polar highs. The intense negative EC-mslp field covered the south subpolar and major parts of south polar with three isolated cores less than -36 mb. Well organized, single positive EC-mslp field occurred over remaining portion of the south polar with core of greater than $+28$ mb.

6.1.4 Departure in mslp

Global distribution of departure from normal broadly resembled the EC-mslp field. The departure was positive over EC-mslp positive field (subtropic and polar) and negative over EC-mslp negative field (subpolar and monsoon regimes). Important to note that negative mslp departure field of Indo-Gangetic plains, western North Pacific, Aleutian Islands, central North America, Iceland, western Europe and Scandinavia formed a continuous stretch of extended intense below normal mslp field (Fig. 10b). Across subtropical through polar region of both the hemispheres, the departure field displayed wavy pattern of alternate positive and negative anomalies with core value ranging from -10 to $+15$ mb over the NH, and from -20 to $+20$ mb over the SH. This

was understandable keeping in view shallower than normal thickness slope from Tibet to north polar, and steeper from Tibet to south polar (Table 3). In brief, spatially connected negative departure field across western equatorial trough, monsoon convergence zone and north subpolar-polar formed a huge and intense low-pressure field, which was surrounded by spatially connected positive departure fields of north and south subtropics as well as that of polars.

6.1.5 Departure in PW

The departure field of PW during 23–28 July 2005 was quite similar to that of normal EC-PW (Fig. 5b). There was mixed distribution of positive and negative PW departures across the globe with isolated core values in the range ± 5 mm.

In order to assimilate global departure field of tropospheric temperature and thickness and mslp, a chart showing the distribution of each of the three departures in two attributes, positive and negative, across 10 subclimatic zones (Table 4) has been prepared (Fig. 11). Based on similarity in the departures, the 10 zones have been grouped into four categories.

(a) *Warmer-thicker troposphere and lower pressure* Entire tropic-subtropic and western north midlatitudes.
(b) *Warmer-thicker troposphere and higher pressure* Eastern north polar and eastern south midlatitudes-south polar.
(c) *Cooler-thinner troposphere and higher pressure* Eastern north midlatitudes, western north and south polars.
(d) *Cooler-thinner troposphere and lower pressure* Western south midlatitudes.

In other words, during 23–28 July 2005, the global atmospheric thermal pattern was divided into four types of temperature departure regimes.

6.2 Actual monsoon and other GWRs, streamlines and departure in wind speed during 23–28 July 2005

At four selected levels (925, 600, 400 and 150 hPa) monsoon regime as well as other GWRs, streamlines and departure from normal in W during 23–28 July 2005 have been shown in Fig. 12 for extended Asia–Pacific region, and Fig. 13 for the globe. The pattern of description given below is similar to that of the normal in the preceding section.

The 3D monsoon structure was well-organized and intense but horizontally spread eastward and southward over western North Pacific and stretched further southeastward across equatorial Pacific (larger portion over the SH). Spreading of the warm-low regime was largest at 1000 hPa (northern Africa, Asia–Pacific and western equatorial
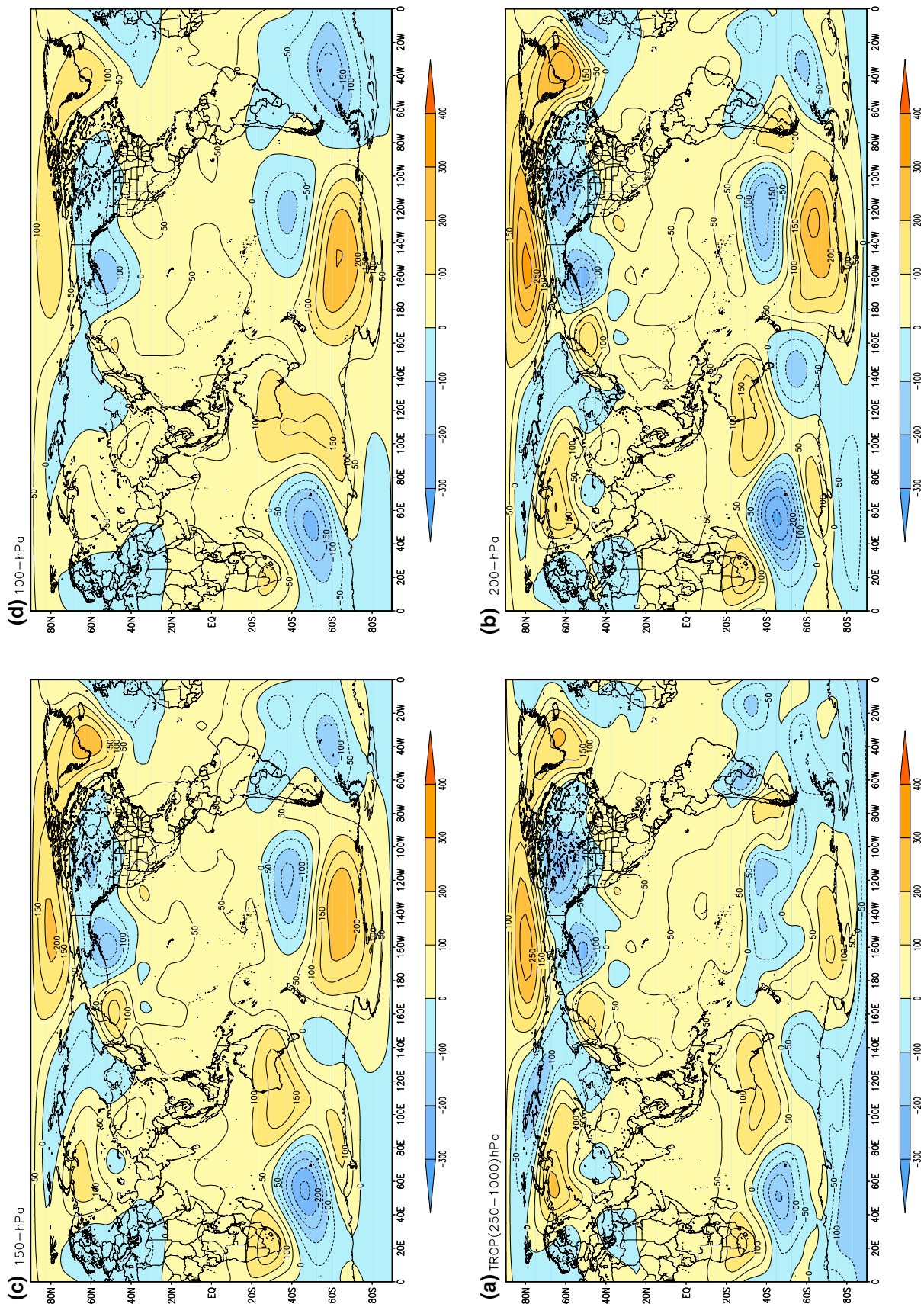
Fig. 9 Chart of 23–28 July 2005 showing global distribution of departure from normal in tropospheric thickness (Z_{TROP}), and that of height of the upper levels (Z_{200}, Z_{150} and Z_{100}. Isolines are in 'm', and yellow shading shows positive departure, and blue negative departure
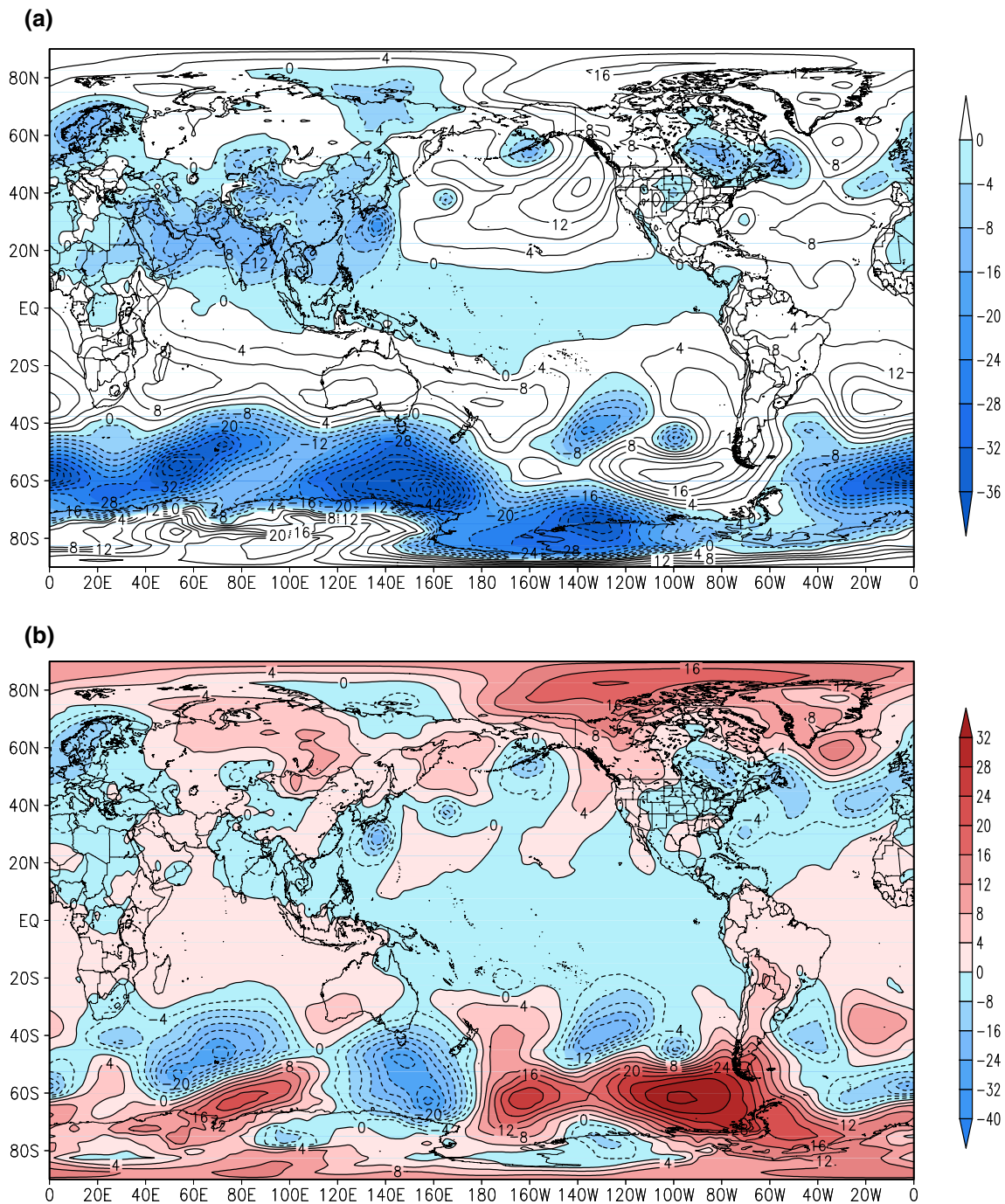
(a)

(b)

Fig. 10 Chart of 23–18 July 2005 showing global distribution of equatorially conditioned mslp (EC-mslp) (**a**) and departure from normal in mslp (**b**). The isolines are in 'mb'. In **a** blue shading shows EC-mslp negative, and unshaded EC-mslp positive; and in **b** red positive departure, and blue negative departure

Pacific) and minimum at 400 hPa around Tibet (Fig. 12). Throughout this depth there were interactions between Eurasian westerlies-turned-northwesterlies and deflected Indo-Pacific equatorial-tropical easterlies across South China–Arabian Sea sector. An extended trough developed across the South China Sea through India at 1000 hPa which gradually reorganized into two well-organized cyclonic circulation at 400 hPa. Warmer-moisture lower tropospheric Indo-Pacific easterlies maintained ample moisture supply to the eastward-southward persistently shifted monsoon circulation. Intense warm-high upper tropospheric anticyclonic circulation was zonally stretched eastward and divided into

Table 4 Departure from normal during 23–28 July 2005 in tropospheric temperature and thickness and mslp over eastern and western sides (with reference to Asia–Pacific) of five broad climatic zones

Geographical domains	Tropospheric temperature T_{TROP} (°C)		Tropospheric thickness Z_{TROP} (m)		mslp (mb)	
	Normal	Departure	Normal	Departure	Normal	Departure
Eastern NPL (north polar) (70°–90°N; 140°E–20°W)	−17.9	+2.4[5%]	10189.2	+114.5[5%]	1010.5	+7.8[5%]
Western NPL (north polar) (70°–90°N; 20°W–140°E)	−16.6	−0.6	10246.5	−20.1	1011.1	+1.3
Eastern NMDLat (north mid-lats.) (45°–70°N; 160°E–60°W)	−11.8	−1.3	10428.2	−57.7	1013.5	+1.4
Western NMDLat (north mid-lats.) (45°–70°N; 60°W–160°E)	−10.2	+1.0	10480.6	+43.4	1009.8	−0.1
Eastern TSBT (tropic–subtropic) (45°S–45°N; 60°E–120°W)	−5.0	+0.9[2%]	10711.2	+40.5[5%]	1013.1	−1.2
Western TSBT (tropic–subtropic) (45°S–45°N; 120°W–60°E)	−5.1	+0.6	10697.3	+24.6	1013.9	−0.7
Eastern SMDLat (south mid-lats.) (45°–70°S; 180°–60°W)	−25.3	+0.1	9858.9	+11.7	998.8	+12.8[2%]
Western SMDLat (south mid-lats.) (45°–70°S; 60°W–180°)	−27.4	−0.6	9788.2	−22.5	992.9	−3.7
Eastern SPL (south polar) (70°–90°S; 180°–60°W)	−37.4	+1.1	9430.3	+44.2	984.9	+9.3
Western SPL (south polar) (70°–90°S; 60°W–180°)	−43.0	−1.3	9221.9	−50.1	1013.5	+5.9
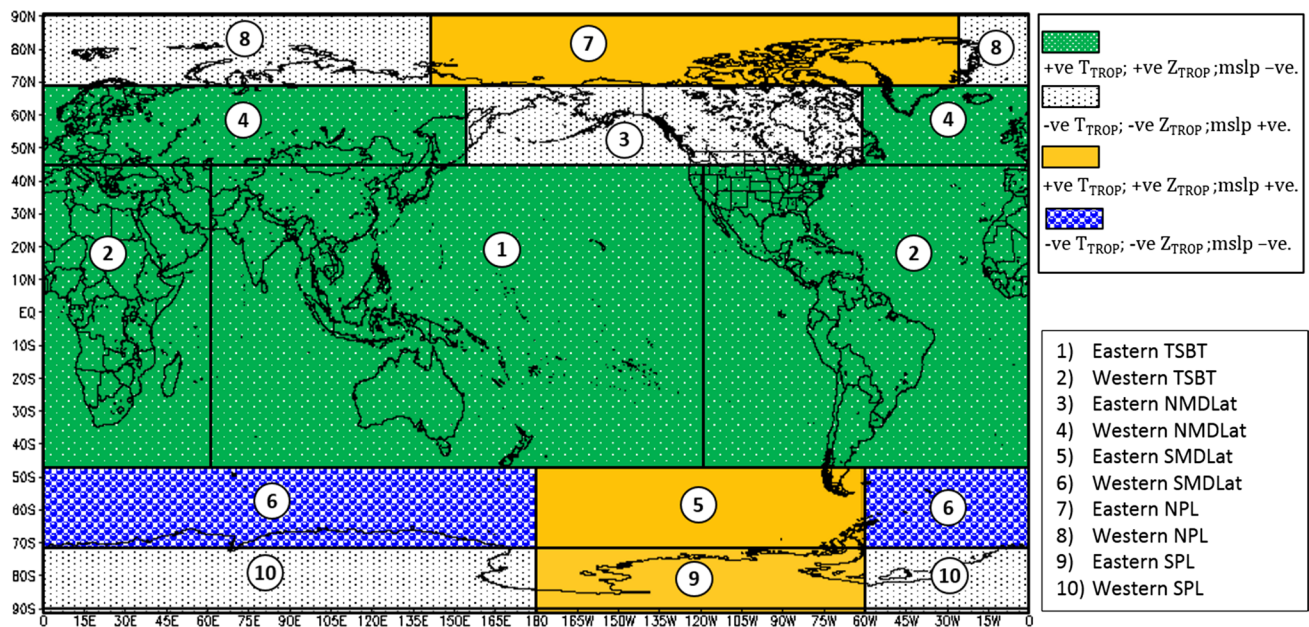
Fig. 11 Demarcation of four types of atmospheric regimes based on departure from normal in T_{TROP}, Z_{TROP} and mslp considered in two attributes (positive and negative) across 10 subclimatic zones of the globe (abbreviation and geographical boundary given in Table 4)

three interconnected cells over Iran, Tibet and western North Pacific. During the 6-day period, a deep cyclonic circulation moved from the Bay of Bengal through central India, shown in Fig. 14. The figure shows 600 hPa streamlines and area under monsoon condition demarcated by applying a provisional criterion: lower–lower tropospheric temperature (1000−700 hPa) and PW higher than the corresponding EMV of the respective parameters, and Z_{600} and mslp lower than the EMV (blue shaded area in Fig. 14). It may be interesting to note that spatial structure of the area under monsoon condition was nearly the same during the 6-Day period. The depth of monsoon circulation and shape and

size of the area under monsoon condition can provide useful guidance about continuity in monsoon rainfall occurrences. Though an extended trough across central India–Bay of Bengal persisted up to 6 August 2005, its intensity was weaker.

West-southwestward directed outflows from upper tropospheric anticyclonic cells while subsiding over northern Africa and adjoining North Atlantic turned toward north polar via anticyclonic curvature and joined the north temperate undulating westerlies with embedded well-organized cyclonic circulation over Scandinavia, Central Asia, Aleutian Islands and northeastern North America–Baffin Sea sector. A portion of the westerlies between levels 850 and
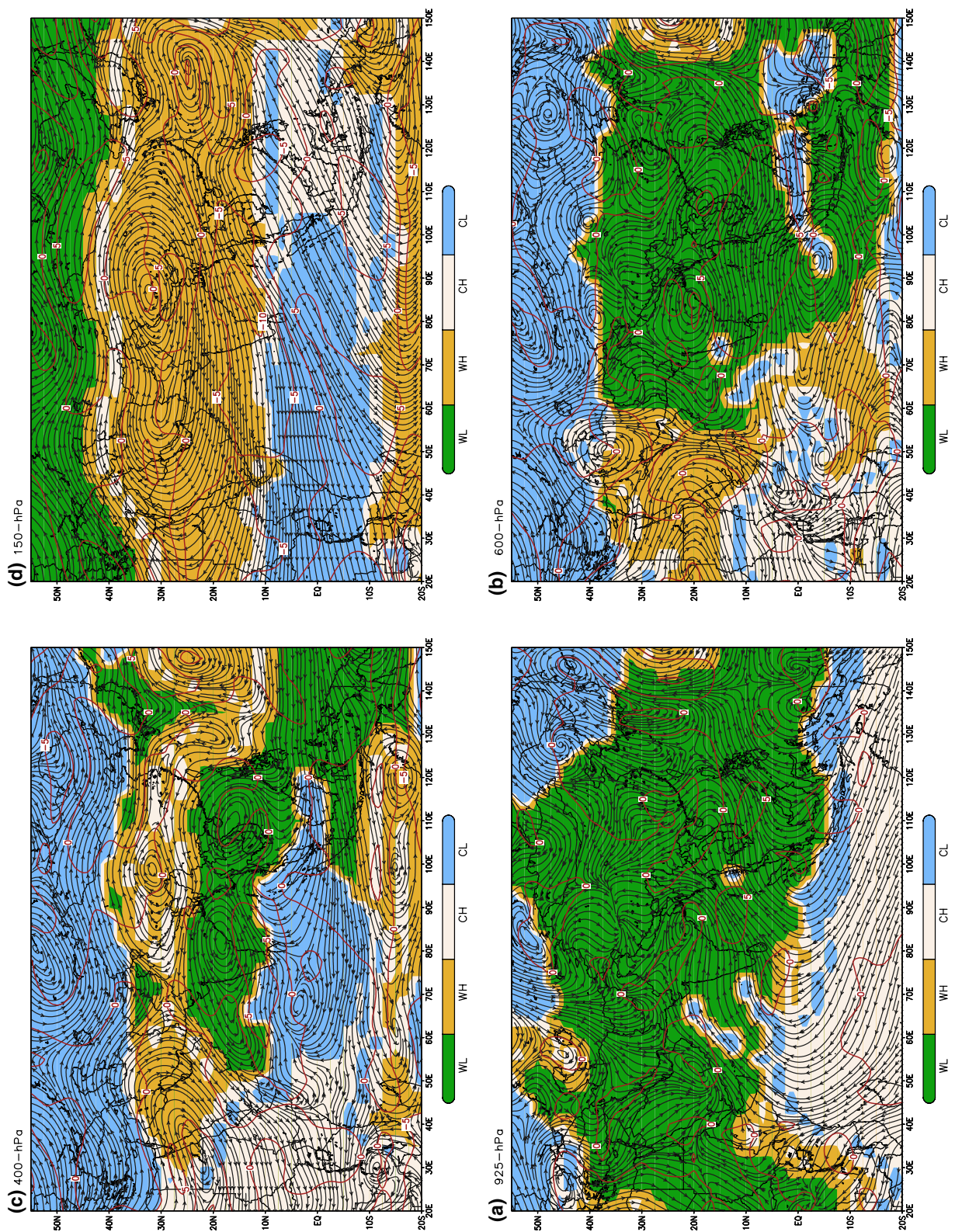
Fig. 12 Chart of 23–28 July 2005 showing actual distribution of GWRs (color shaded), streamline and departure from normal in *W* (m/s, red isolines) at 925-hPa (**a**), 600-hPa (**b**), 400-hPa (**c**) and 150-hPa (**d**) over extended Asia–Pacific region. Green shading shows *WL* warm-low regime; orange shading shows *WH* warm-high regime; white shading shows *CH* cool-high regime; blue shading shows *CL* cool-low regime
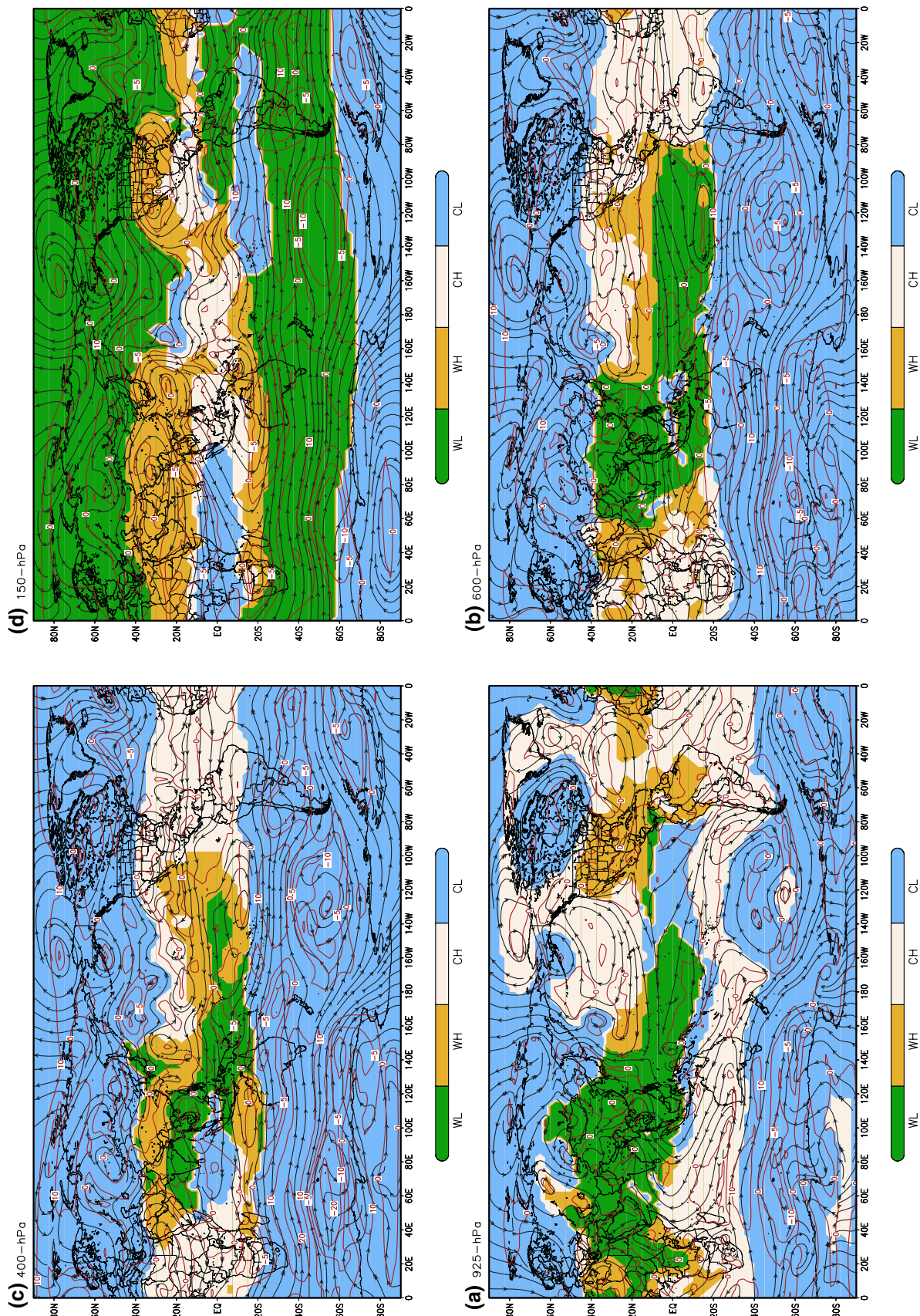
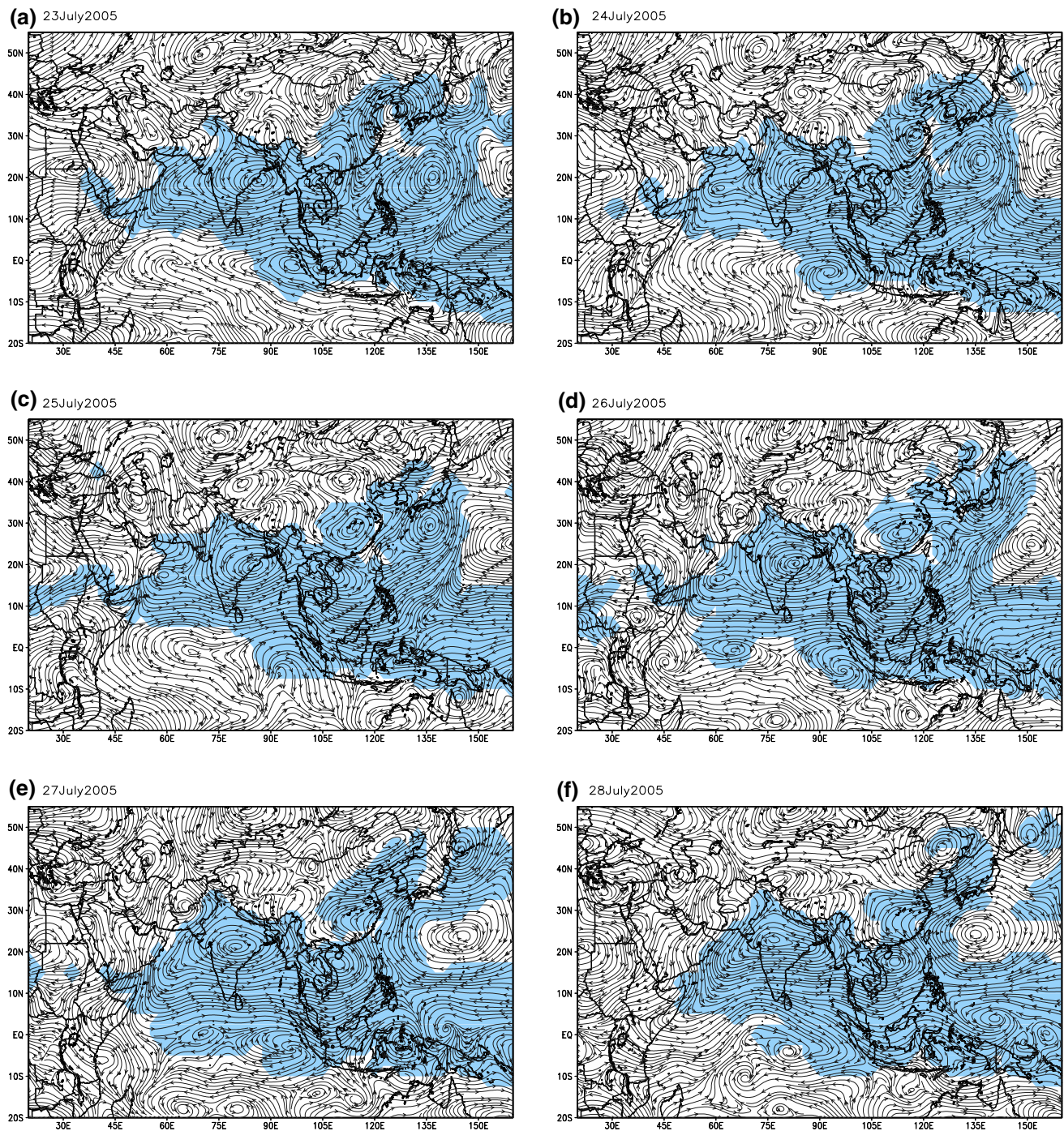**Fig. 13** Same as in Fig. 12 but over the globe

Fig. 14 The 600-hPa streamlines for each day of the 6-day rainstorm period (23–28 July 2005). Blue color coding indicates area under monsoon condition demarcated by applying the criteria: lower tropospheric temperature (1000−700 hPa) and PW higher than corresponding EMV, and Z_{600} and mslp lower than the EMV

400 hPa entered into monsoon domain and converged into cyclonic circulation over central India. Further, a portion of Eurasian westerlies in the troposphere was diverted toward north polar due to warmer-thicker troposphere over North Pacific which formed an anticyclonic circulation over Arctic Ocean (north of Russia–Alaska −Canada sector). The

Eurasian westerlies advected sensible heat from warmer tropic-subtropic regions as well as excessive latent heat of condensation released during the heaviest rainstorm over India caused warmer and thicker troposphere and higher pressure over the Arctic Ocean. Northeasterly return-flows from this polar high after colliding and converging with

zonally flowing westerlies intensified the Aleutian convergence and deepened subpolar low there. The rising airs from the cool-low Aleutian low via North Pacific high and equatorial-tropical easterlies eventually converged into the monsoon regime. Over cooler western side of the north polar (with reference to Asia–Pacific), there was development of a cyclonic circulation adjacent to the eastern Arctic Ocean high covering the remaining portion of the Arctic Ocean. From the upper tropospheric anticyclonic circulation, lesser outflows were directly blowing toward north polar, consequently, upper levels of the eastern Arctic Ocean anticyclone were cooler than normal. Higher geopotential height of the upper levels was due to warmer-thicker troposphere underneath. The height was an integrated parameter with positive height departure of the lower levels. Important to note that tropospheric temperature and thickness slope was shallower than normal from Tibet-to-north polar and steeper from Tibet-to-south polar. The greater portion of the outflows, particularly from anticyclonic cells over Tibet and western North Pacific, was directed southwards. Due to channelization of this larger volume of flow, the 150 hPa TEJ was stronger than normal (+ 5 m/s) and eastward shifted over the equatorial Indian Ocean. After crossing the equator and partly subsiding over south subtropical highs, a part of the outflows flowed with south midlatitude undulating westerlies keeping warmer than normal air on the left and cooler on the right. Due to warmer-thicker troposphere over the South Pacific Ocean, the westerlies were diverted toward south polar where warmer-thicker troposphere, anticyclonic circulation and higher pressure developed on eastern side of the south polar and cooler-thinner troposphere, cyclonic circulation and lower pressure on western side.

The core of the departure field in W over the NH was located over subpolar-polar regions. In the core, departure in W was $+5$ m/s at 1000 hPa, increased to $+20$ m/s at 250 hPa and then decreased to $+5$ m/s at 100 hPa. Over the SH, there were two cores located over subtropical Indian and Pacific Oceans. In the core, the departure was $+10$ m/s at 1000 hPa, $+25$ m/s at 250 hPa, and again $+10$ m/s at 100 hPa.

6.3 Departure in temperature, height and circulation of the upper levels during 23–28 July 2005

Based on positive and negative departure in temperature and height of the upper levels (200, 150 and 100 hPa) (Table 5), the ten 10 subclimatic zones can be grouped in three categories.

(a) *Warmer atmosphere and higher height* (*tropic-subtropic, western north polar and western south polar*) Tropic-subtropic accounts more than 70% surface area of the globe. Increase in tropospheric temperature and thickness over the zone caused increased convection and rise in temperature and height of the upper levels.

(b) *Warmer atmosphere and lower height* (*eastern north midlatitude and western south midlatitude*) Advected heat by the upper tropospheric anticyclonic airflows was accumulated due to upper level cyclonic circulation and slow subsidence over the zones. Due to accumulation of heat, temperature increased but height remained lower as it was an integrated parameter with the height of the lower levels.

(c) *Cooler atmosphere and higher height* (*western north midlatitude, eastern north polar, eastern south midlatitude and eastern south polar*) Over these subzones, troposphere (1000–250 hPa) was warmer and thicker due to warmer outflows while subsiding either flowed through them or formed anticyclonic circulation and higher-pressure field. Directly lesser outflows reached to upper levels of these subzones, therefore, temperature was lower but height higher due to its integration with height of the lower levels.

Table 5 Departure from normal during 23–28 July 2005 in upper levels temperature and height over the 10 subclimatic zones

Geographical domains	T_{200}	T_{150}	T_{100}	Z_{200}	Z_{150}	Z_{100}
Eastern NPL (north polar)	$-4.9^{1\%}$	$-3.2^{1\%}$	$-2.8^{1\%}$	$+149.6^{1\%}$	$+116.7^{2\%}$	$+82.4^{10\%}$
Western NPL (north polar)	$+1.0$	$+0.1$	-0.3	$+5.7$	$+8.8$	$+7.6$
Eastern NMDLat (north mid-lats.)	$+1.6$	$+0.5$	$+0.1$	-40.4	-31.8	-28.4
Western NMDLat (north mid-lats.)	-1.0	$-1.2^{10\%}$	-1.0	$+42.2$	$+33.2$	$+20.1$
Eastern TSBT (tropic–subtropic)	$+1.4^{5\%}$	$+0.4$	-1.1	$+40.4^{10\%}$	$+48.2^{5\%}$	$+45.1^{10\%}$
Western TSBT (tropic–subtropic)	$+0.4$	0	-0.7	$+24.2$	$+26.2$	$+21.0$
Eastern SMDLat (south mid-lats.)	-1.2	-1.4	-0.9	$+104.1^{10\%}$	$+94.1$	$+79.8$
Western SMDLat (south mid-lats.)	$+1.9$	$+0.8$	$+0.8$	-32.8	-20.2	-12.3
Eastern SPL (south polar)	-0.5	-0.5	-1.0	$+94.4$	$+91.4$	$+81.5$
Western SPL (south polar)	$+0.4$	$+0.6$	-0.2	-4.3	$+1.6$	$+2.5$

For geographical boundary see Table 4

7 Summary and conclusions

In the study, investigation has been carried to understand departure from normal in global atmospheric thermal condition, and 3D structure of monsoon and general atmospheric circulations during the heaviest wet spell (23–28 July 2005). Atmospheric condition has been described with respect to equatorial mean as reference, and a premise advanced to define and describe 3D structure of monsoon as well as general atmospheric circulations.

7.1 Normal condition during 23–28 July

During 23–28 July, the troposphere is cooler/thinner-than-equator over the NH by − 2.3 °C/− 116.2 m and the SH by − 11.9 °C/− 494.8 m. It is warmest/thickest over the Tibetan plateau (+ 7.9 °C/+ 167.5 m). The north–south tropospheric temperature/thickness contrast is positive and strong (+ 9.6 °C/+ 378.5 m). The EC-T_{TROP}/EC-Z_{TROP} decreases monotonically towards polars—less than − 22.2 °C/− 605.5 m over north polar and − 38.6 °C/− 1528.8 m over south polar. Around this time of the year, a huge contiguous negative EC-mslp field develops around Tibetan region, which is surrounded by intense positive EC-mslp field of spatially connected subtropical and polar highs. In this backdrop of atmospheric condition, the monsoon circulation attains maturity. Precipitable water across Asia–Pacific is higher than the equator (41.4 mm). In the core over the head Bay of Bengal and eastern-northeastern India, the EC-PW exceeds + 20 mm.

Centered around Tibetan region, the Asia–Pacific monsoon is the biggest barotropic weather system with largest-thickest warm-low-moist lower tropospheric convective-confluence convergence extending up to 500 hPa over Indo-Gangetic plains, and largest warm-high upper tropospheric divergence with vertical depth extending beyond 100 hPa over subtropical Afro-Eurasia. Up to 850 hPa, deflected Indo-Pacific easterlies sweep the entire Asia–Pacific region. In the layer 850−500 hPa, Eurasian westerlies-turned-northwesterlies enter into Indian subcontinent and evolve into a giant whirlpool-type cyclonic circulation. Intense interactions between deflected Indo-Pacific easterlies and Eurasian northwesterlies cause generation of secondary perturbations (eddy, cyclonic circulation, trough, etc.), moist convergence and rainfall. Outflows from upper tropospheric anticyclonic circulation subside over subtropical and polar highs, and return-flows from lower levels of the highs through a variety of meander courses eventually converge in monsoon warm-low regime. The outflows from upper tropospheric circulation that are directed southwards are forced to pass through a relatively narrow passage between Tibetan anticyclonic and equatorial anticyclonic circulations where channelization effects produce famous 'TEJ'. The 150 hPa GC-*W* exceeds + 10 m/s in the core area of the TEJ over the equatorial Indian Ocean–African sector'. Outside the monsoon regime, atmospheric dynamism is subdued through the full depth of northern troposphere, and intense through the southern troposphere.

7.2 Perturbed condition during 23–28 July 2005

Considering departure from normal in tropospheric temperature and thickness and mslp during 23–28 July 2005 in two attributes, positive and negative, the ten subclimatic zones were grouped in four categories.

(a) *Warmer-thicker troposphere and lower pressure* Entire tropic-subtropic and western north midlatitudes.
(b) *Warmer-thicker troposphere and higher pressure* Eastern north polar and eastern south midlatitudes-south polar.
(c) *Cooler-thinner troposphere and higher pressure* Eastern north midlatitudes, western north and south polars.
(d) *Cooler-thinner troposphere and lower pressure* Western south midlatitudes.

Noticeable changes in 3D monsoon structure were: horizontally spread eastward-southward over western North Pacific, and stretched further southeastward and across equatorial Pacific (larger stretching on southern side); intense warm-low lower tropospheric confluence-convergence across Asia–Pacific with vertical depth extended up to 400 hPa; and intense warm-high upper tropospheric anticyclonic circulation zonally stretched and divided into three interconnected cells across Iran–Tibet–western North Pacific. Warmer-moisture lower tropospheric Indo-Pacific easterlies maintained ample moisture supply to the eastward-southward shifted monsoon circulation persistently. During the period, a deep cyclonic circulation moved from Bay of Bengal through central India. An extended but weaker trough across central India–Bay of Bengal persisted up to 6 August 2005. Outflows from upper tropospheric anticyclonic cells broadly followed three pathways, westward/southwestward, northeastward/eastward and southward. At 150-hPa, the 'TEJ' was stronger (+5 m/s) and eastward shifted over the equatorial Indian Ocean. Westward/southwestward directed outflows while subsiding over northern Africa and North Atlantic turned right, joined north midlatitude westerlies, flowed over Eurasia, drifted northward and eventually produced warmer-thicker troposphere, anticyclonic circulation and higher pressure over eastern north polar, and cooler-thinner troposphere, cyclonic circulation and higher pressure over western north polar. Part directed

northeastward/eastward mostly subsided over eastern north midlatitudes (northern North Pacific) and produced cooler-thinner troposphere, cyclonic circulation and higher pressure there. In other words, lesser flow reached to eastern north polar, consequently, upper levels were cooler. Major parts of the outflows were directed southwards. A portion subsided over south subtropical highs while remaining flowed as south midlatitude westerlies, which produced warmer-thicker troposphere, deep anticyclonic circulation and higher pressure over eastern south midlatitude-polar sector, and cooler-thinner troposphere, upper level cyclonic circulation and lower level anticyclonic circulation and higher pressure over western south polar. Return-flows from the south polar high(s) collided and converged with midlatitude westerlies and produced cooler-thinner troposphere, cyclonic circulation and intense convergence over western south midlatitudes.

Persistent warmer-thicker tropospheric over tropic-subtropic, well-organized, more prominent and statistically significant (at 5% level) over eastern tropic-subtropic (Pacific region), and greater warming over east of eastern Tibet and lesser westward during 23–28 July 2005 produced persistent moderate increase in regional (Asia–Pacific) monsoon circulation and subregional extreme wet spell 23–28 July 2005 and extreme rainwater on 25 July 2005 over India and local extreme rainfall on 27 July 2005 at Mumbai. Intense monsoon circulation in turn advected sensible heat from warmer tropic-subtropic regions as well as the latent heat of condensation released during the heaviest rainstorm, which warmed and thickened the troposphere over western north midlatitudes, eastern north polar (significant at 5% level) and eastern south midlatitude-polar sector. Monitoring 3D global thermal condition and general atmospheric as well as monsoon circulations can provide useful guidance to users to understand the cause of rainfall activity, its severity, and likely continuity.

References

Ajayamohan RS, Merryfield WJ, Kharin VV (2010) Increasing trend of synoptic activity and its relationship with extreme rain events over Central India. J Clim 23:1004–1013

Bohra AK et al (2006) Heavy rainfall episode over Mumbai on 26 July 2005. Assessment of NWP guidance. Curr Sci 90(9):1188–1194

De US, Dutta S (2005) West coast rainfall and convective instability. J Ind Geophys Union 9(1):71–82

Durman CF, Gregory JM, Hassell DC, Jones RG, Murphy JM (2001) The comparison of extreme European daily precipitation simulated by a global and a regional climate model for present and future climates. Q J R M S 127:1005–1015

Francis PA, Gadgil S (2006) Intense rainfall events over the west coast of India. Meteorol Atmos Phys 94:27–42

Goswami P, Ramesh KV (2008) Extreme rainfall events: vulnerability analysis for disaster management and observation system design. Curr Sci 94(8):1037–1044

Goswami BN, Venugopal V, Sengupta D, Madhusoodanan MS, Xavier PK (2006) Increasing trend of extreme rain events over India in a warming environment. Science 314:1442–1445

Guhathakurta P, Sreejith OP, Menon PA (2011) Impact of climate change on extreme rainfall events and flood risk in India. J Earth Syst Sci 120(3):359–373

Hunt JCR, Burgers JM (2002) Floods in a changing climate: a review. Phil Trans R Soc Lond A 360:1531–1543

IPCC (2007) Climate change 2007. The physical science basis. The contribution of working group I to the fourth assessment report of the intergovernmental panel on climate change. Cambridge University Press, Cambridge, pp 504–511

Kharin VV, Zwiers FW (2000) Changes in the extreme in an ensemble of transient climate simulations with a coupled atmosphere-ocean GCM. J Climate 13:3760–3788

Klein Tank AMG et al (2006) Changes in daily temperature and precipitation extremes in Central and South Asia. J Geophys Res 111:D16105. https://doi.org/10.1029/2005JD006316

Kumar A, Didhia J, Rotunno Niyogi D, Mohanty UC (2008) Analysis of the 26 July 2005 heavy rain event over Mumbai, India using the weather research and forecasting (WRF) model. Q J R Meteorol Soc 134:1897–1910

Kundzewicz ZW, Rosbjerg D, Simonovic SP, Takeuchi K (eds) (1993) Extreme hydrological events: precipitation, floods, and droughts. IAHS Publication No. 213. IAHS, Wallingford, p 74

NDMG (National Disaster Management Guidelines) (2008) Management of floods. National Disaster Management Authority, New Delhi

Qian W, Lee DK (2000) Seasonal march of Asian summer monsoon. Int J Climatol 20:1371–1386

Rajeevan M, Bhate J (2008) A high resolution daily gridded rainfall Data Set (1971–2005) for Mesoscale Meteorological Studies. National Climate Center, India meteorological Department, research report No.9

Rajeevan M, Bhate Jyoti, Jaswal AK (2008) Analysis of variability and trends of extreme rainfall events over India using 104 years of gridded daily rainfall data. Geophys Res Lett 35:L18707

Rama Rao YV, Hatwar HR, Salah AK, Sudhakar Y (2007) An experiment using the high-resolution Eta and WRF models to forecast heavy precipitation over India. Pure Appl Geophys 164:1593–1615

Ramage CS (1971) Monsoon Meteorology. International geophysics series, 15th edn. Academic Press, New York, p 290

Ranade A (2010) Studies on hydrological wet season and occurrence of dry and wet spells over river basins of India. Ph.D. thesis, Atmospheric and Space Sciences, University of Pune, India, p 372

Ranade A, Singh N (2014) Large-scale and spatio-temporal extreme rain events over India: a hydrometeorological study. Theor Appl Climatol 115:375–390

Ranade A, Singh N, Singh HN (2010) Effect of La Niña-El Niño on climatic fluctuations over major hydro-ecozones across India. J Hydrol Res Devp 25:13–36

Saha S et al (2010) The NCEP climate forecast system reanalysis. Bull Am Meteorol Soc 91(8):1015–1057. https://doi.org/10.1175/2010BAMS3001.1

Saha S et al (2014) The NCEP climate forecast system version 2. J Climate 27:2185–2208. https://doi.org/10.1175/JCLI-D-12-00823.1

Sen Roy S, Balling RC (2004) Trends in extreme daily precipitation indices in India. Int J Climatol 24:457–466

Senior CA, Jones RG, Lowe JA, Durman CF, Hudson D (2002) Predictions of extreme precipitation and sea-level rise under climate change. Phil Trans R Soc Lond A 360:1301–1311

Shyamala B, Bhadram CVV (2006) Impact of mesoscale-synoptic scale interactions on the Mumbai historical rain event during 26–27 July 2005. Curr Sci 91(12):1649–1654

Sikka DR, Rao PS (2008) The use and performance of mesoscale models over the Indian region for two high-impact events. Nat Hazards 44:353–372

Singh N, Ranade A (2010) The wet and dry spells across India during 1951–2007. J Hydrometeorol 11:26–45

Strahler A (2011) Introducing physical geography, 5th edn. Wiley, New Jersey

Vaidya SS, Kulkarni JR (2007) Simulation of heavy precipitation over Santacruz, Mumbai on 26 July 2005, using mesoscale model. Meteorol Atmos Phys 98:55–66

Zwiers FW, Kharin VV (1998) Changes in the extremes of the climate simulated by CCC GCM2 under CO_2 doubling. J Climate 11:2200–2222